

Bring the Heat: Tidal Heating Constraints for Black Holes and Exotic Compact Objects from the LIGO-Virgo-KAGRA Data

Horng Sheng Chia^{1a}, Zihan Zhou^{2b}, and Mikhail M. Ivanov^{3c}

¹ *School of Natural Sciences, Institute for Advanced Study, Princeton, NJ 08540, USA*

² *Department of Physics, Princeton University, Princeton, NJ 08540, USA*

³ *Center for Theoretical Physics, Massachusetts Institute of Technology, Cambridge, MA 02139, USA*

Abstract

We present the first constraints on tidal heating for the binary systems detected in the LIGO-Virgo-KAGRA (LVK) gravitational wave data. Tidal heating, also known as tidal dissipation, characterizes the viscous nature of an astrophysical body and provides a channel for exchanging energy and angular momentum with the tidal environment. Using the worldline effective field theory formalism, we introduce a physically motivated and easily interpretable parametrization of tidal heating valid for an arbitrary compact astrophysical object. We then derive the imprints of the spin-independent and linear-in-spin tidal heating effects of generic binary components on the waveform phases and amplitudes of quasi-circular orbits. Notably, the mass-weighted spin-independent tidal heating coefficient derived in this work, \mathcal{H}_0 , is the dissipative analog of the tidal Love number. We constrain the tidal heating coefficients using the public LVK O1-O3 data. Our parameter estimation study includes two separate analyses: the first treats the catalog of binary events as binary black holes (BBH), while the second makes no assumption about the nature of the binary constituents and can therefore be interpreted as constraints for exotic compact objects. In the former case, we combine the posterior distributions of the individual BBH events and obtain a joint constraint of $-13 < \mathcal{H}_0 < 20$ at the 90% credible interval for the BBH population. This translates into a bound on the fraction of the emitted gravitational wave energy lost due to tidal heating (or gained due to radiation enhancement effects) at $|\Delta E_H/\Delta E_\infty| \lesssim 3 \cdot 10^{-3}$. Our work provides the first robust framework for deriving and measuring tidal heating effects in merging binary systems, demonstrating its potential as a powerful probe of the nature of binary constituents and tests of new physics.

Email: ^ahschia@ias.edu, ^bzihanz@princeton.edu, ^civanov99@mit.edu

Contents

1	Introduction	1
2	Summary of Main Results	4
3	Tidal Heating Effects on Gravitational Waves: Theory	7
3.1	Worldline EFT for Tidal Heating of a Non-Rotating Body	8
3.2	Tidal Heating of a Rotating Compact Body	11
3.3	Estimates for Tidal Dissipation Coefficients	15
3.4	Tidal Heating Imprints on Waveforms	16
3.5	Simplified Waveforms for Binary Black Holes	19
4	Constraints on Tidal Heating from LVK O1-O3 Data	20
4.1	Inspirational-Merger-Ringdown + Dissipation for Binary Black Holes	20
4.1.1	Constraints for Individual Events	21
4.1.2	Constraints at the Population Level	21
4.2	Inspirational-only + Dissipation for Exotic Binaries	26
5	Conclusions and Outlook	28
A	Derivation of Waveform Observables	30
	References	38

1 Introduction

Gravitational wave (GW) science is a precision science. In the current growing era of GW astronomy, in which the LIGO-Virgo-KAGRA (LVK) detector network routinely detects orbiting binary black holes [1–14], the need for highly accurate and precise waveforms is increasingly apparent in order to achieve a wide range of GW science. To this end, one active area of research involves computing ever higher post-Newtonian (PN) terms for the waveform observables of merging binary systems [15–20]. In this approach, a binary system is often first modeled as orbiting point particles, with their intrinsic parameters described by the component masses and spins. Moving beyond the point-particle approximation, various so-called finite-size effects which characterize the underlying multipolar structure of the binary constituents are incorporated in the waveform models. These finite-size effects include the spin-induced moments [21–30], the tidal deformability [31–38] and the tidal heating [39–48] of the astrophysical bodies — all of which would impact GW observables in non-trivial ways. In this paper, we conduct a comprehensive study on the imprints of tidal heating of general astrophysical bodies on GW observables. Our study *a priori* makes no assumption about the nature of the compact objects, and is therefore applicable to both binary black holes (BBH) and other general exotic types of compact binaries.

Tidal heating [39–48], also commonly referred to as tidal dissipation, captures the viscosity of an astrophysical body and serves as an important channel for exchanging energy and angular momentum between the body and its external tidal environment. Perhaps the most familiar example of this effect lies literally at our cosmic backyard: the Earth-Moon system. In this case, the misalignment between the tidal bulge of the oceans on Earth and the radial separation between the Earth-Moon center of masses generates frictional forces that transfer energy and angular

momentum between the two bodies and the orbit [47–49]. This process ultimately leads to tidal locking, whereby the rotational frequency of the Moon synchronizes with its orbital frequency around Earth, and is the reason why we only see one side of the Moon [47–49]. In addition to this well-known example, tidal dissipation is also responsible for a plethora of interesting astrophysical phenomena. For black holes orbiting around large companion stars, tidal heating has been invoked as a potential mechanism for spinning up the black holes [50–54], ultimately forming merging BBHs with at least one highly-spinning component which may be observable by the LVK detectors [55–59]. Tidal dissipation is also directly responsible for a remarkable phenomenon known as black hole superradiance [60–67], in which energy and angular momentum may be extracted from a rotating black hole if its spin is sufficiently high compared to the angular phase velocity of its surrounding perturbation field. Black hole superradiance has therefore been proposed as a powerful probe of ultralight dark matter [68–74], as it could spontaneously form bosonic condensates around the black holes and produce a wealth of interesting astrophysical signatures [75–84]. Owing to the unique nature of the event horizon, any potential departures of the black hole tidal heating effects in extreme-mass-ratio systems have also been proposed as signs of modifications of General Relativity or the existence of heavy exotic compact objects in the Universe [85–88].

While the physical imprints of other finite-size effects, such as the spin-induced moments [21, 23, 24, 26–30] and the tidal deformability [31–38], of a general body on GWs have been studied extensively in the literature, the same cannot be said for tidal heating. This relative lack of progress stems primarily from the absence of a rigorous, first-principle derivation of this effect for a general astrophysical body on GW observables. To date, studies on tidal heating for a general body are either restricted to the Newtonian limit [89] or adopt a phenomenological approach [86, 87, 90–92], whereby the GW phases and amplitudes are artificially deformed at the PN orders at which tidal dissipation are known to appear. In the latter case, ad-hoc parameters have been introduced to model tidal dissipation at 2.5PN and 3.5PN orders for rotating bodies and at 4PN for non-rotating bodies. Such parameterizations, while enabling some examination of this effect on GW observables, cannot be directly mapped to physical quantities such as the energy flux absorbed by the body. Moreover, to the best of our knowledge, most studies involving tidal heating in the context of data analysis have only been performed at the level of Fisher analyses of waveform mismatch [86, 87, 90–92] but have not been applied to real data for parameter estimations studies (though see [93] for recent result on tidal heating constraints the binary neutron star GW170817).

In this paper, we expand upon previous investigations on tidal heating on both the theoretical frontier and from a data analytical perspective. On the theoretical front, we present a rigorous modeling of tidal dissipation of a single body by adopting the worldline effective field theory (EFT) formalism [22, 32, 94–100] (see [101–104] for recent reviews). In the EFT framework, tidal dissipation can be described by a set of free coefficients in the non-local part of the retarded tidal response function of a compact body. These coefficients appear in front of operators whose structure is fully dictated by symmetries. EFT offers a systematic approach towards modeling both the spin-dependent and spin-independent tidal dissipation effects. Furthermore, this formalism *a priori* makes no assumption about the nature of the binary components and is therefore applicable to all types of astrophysical bodies.

With the EFT, physically-motivated parameterizations of tidal heating for a general binary system can be derived in a straight forward manner. For binary systems with non-spinning components, we find that the leading-order tidal dissipation coefficient is described by the mass-weighted parameter \mathcal{H}_0 – see (2.6) for its definition – and first appears at 4PN order in waveform observables. \mathcal{H}_0 can be thought of as a generalization of the Newtonian viscous lag time scale. It is worth emphasizing that \mathcal{H}_0 is the dissipative counterpart of the more well-known effective tidal Love parameter describing the conservative tidal deformation, which is often denoted by $\tilde{\Lambda}$ in the literature [33, 105].¹ For binary systems with spinning components, the leading-order tidal heating parameters first appear at 2.5PN order, and they are defined in (2.7). Physically, they measure the body’s angular velocity. In the EFT, their origin can be traced back to the transformation from the co-rotating frame to the local inertial frame. Thus, EFT automatically incorporates possible radiation enhancement effects such as superradiance. While it is well known that the spin-independent and spin-dependent tidal heating terms first appear at 4PN and 2.5PN orders respectively, our derivation provides a first-principles derivation of the functional form of the physically-motivated effective dissipation numbers in binary systems. Since the effective dissipation numbers described in this paper can be directly mapped to the microscopic properties of orbiting bodies, their measurements or constraints thereof provide meaningful physical interpretations on the nature of the binary sources.

In addition to the theoretical investigation of tidal heating, we also present the parameter estimation (PE) constraints on the dissipation numbers using the public LVK data. Crucially, we present our constraints for both binary black holes and for exotic compact objects — in the former case, we exploit various properties which are unique to black holes, such as the black hole electric-magnetic duality [94, 95, 107, 109, 120–122], to obtain stronger PE constraints; while in the latter we make no such assumptions and therefore constrain all of the different dissipation numbers simultaneously in the PE process. Interestingly, although the spin-dependent effective numbers (2.7), and the higher order terms thereof, formally appear at lower PN orders compared to the 4PN spin-independent coefficient (2.6), we found that the spin-independent coefficient \mathcal{H}_0 is best constrained as the spins of most detected BBHs are not very precisely measured and are largely consistent with zero [56, 58, 59]. While the current constraints on \mathcal{H}_0 for black holes is approximately two orders of magnitude larger than the theoretical prediction from General Relativity, future GW observations will rapidly improve the constraints as the detectors’ sensitivity improves and the number of binary detection increases. All in all, this work presents the first rigorous derivation of tidal heating effects on GW observables using the EFT approach and provides the first physically-motivated constraints of tidal heating of GW sources.

Outline: In Section 2 we present a summary and the main results of this work. In Section 3 we study the theoretical aspects of tidal dissipation for a general rotating body and its impact on GW observables of binary systems. In Section 4 we apply our theoretical results to the public LIGO-Virgo-KAGRA data and constrain the various dissipation numbers of the detected binary systems. Here we separate our analyses into two parts: the first assumes that the binaries are binary black holes, while the second relaxes this assumption and therefore applies to all kinds

¹The tidal Love numbers have recently been a subject of intense theoretical research, especially in the context of black holes, see e.g. [35, 36, 97, 99, 106–119].

of exotic compact objects. We present our conclusions and outlook in Section 5. Details of the derivations for the waveform observables are shown in Appendix A.

Notations and Conventions: We use the superscript ^{src} to distinguish source-frame and detector-frame quantities. For instance, the source-frame chirp mass is denoted by \mathcal{M}^{src} whereas the detector-frame chirp mass is \mathcal{M} . Latin letters $\{i, j, k\}$ denote spatial indices. We use m_ℓ to denote the azimuthal angular momentum number in order to avoid confusion with the component mass m . We adopt the following conventions for several convenient mass and spin quantities:

$$\begin{aligned} M &:= m_1 + m_2 & \eta &:= m_1 m_2 / M^2 & \delta &:= (m_1 - m_2) / M \\ \chi_i &:= \mathbf{S}_i / m_i^2 & \chi_s &:= (\chi_1 + \chi_2) / 2 & \chi_a &:= (\chi_1 - \chi_2) / 2 \end{aligned} \tag{1.1}$$

where \mathbf{S}_i is the component spin angular momentum and χ_i is the dimensionless spin.

2 Summary of Main Results

Tidal effects probe the internal structure of a compact astrophysical body beyond the point particle approximation. In the post-Newtonian (PN) regime, the leading order tidal effect on the gravitational waveforms stems from tidal heating (4PN for non-rotating bodies and 2.5PN for spinning ones). The LVK GW data is usually analyzed under the “standard physics” assumption that detection triggers whose binary component masses are above $\approx 3M_\odot$ correspond to black hole-black hole mergers in general relativity. Based on the PN counting, deviations from this scenario, if any, are expected to first show up at the level of tidal heating parameters. In this work, we demonstrate how to use these leading order effects to test the nature of compact relativistic objects with GW data. Our work is a natural extension of the efforts to probe the nature of astrophysical compact objects with conservative tidal deformations, parameterized by static Love numbers. The effects of Love numbers, however, first appear at 5PN, and hence we expect the tidal heating effects to provide a stronger test of new physics from a PN counting perspective. Note that the Love numbers of exotic compact objects have been constrained with LVK data earlier in [12].

We derive the constraints on tidal heating of black holes and black hole-like exotic compact objects using the LIGO-Virgo O1-O3 gravitational wave merger catalogs [1–14]. To this end, we carry out two types of analyses. In our baseline analysis we place bounds on tidal heating of black holes, assuming the electric-magnetic duality that is satisfied by black holes in four dimensional general relativity [94, 95, 107, 109, 120–122]. This analysis effectively tests whether dissipation properties of black holes in the LVK data is consistent with general relativity. In the second analysis, for each LVK event normally interpreted as a black hole - black hole merger, we derive bounds on a generic set of tidal heating parameters of the binary components. This effectively constrains exotic compact objects whose tidal properties are different from those of black holes.

We use the worldline effective field theory (EFT) [22, 32, 94–100] to describe effects of tidal heating and dissipation on the gravitational waveforms. EFT allows one to parametrize these effects in a model-independent fashion, using symmetry arguments only. We show that at the first non-trivial order in spin and frequency, these effects are captured by two free parameters, which can be thought of as generalizations of the tidal Love numbers. These parameters are defined as follows.

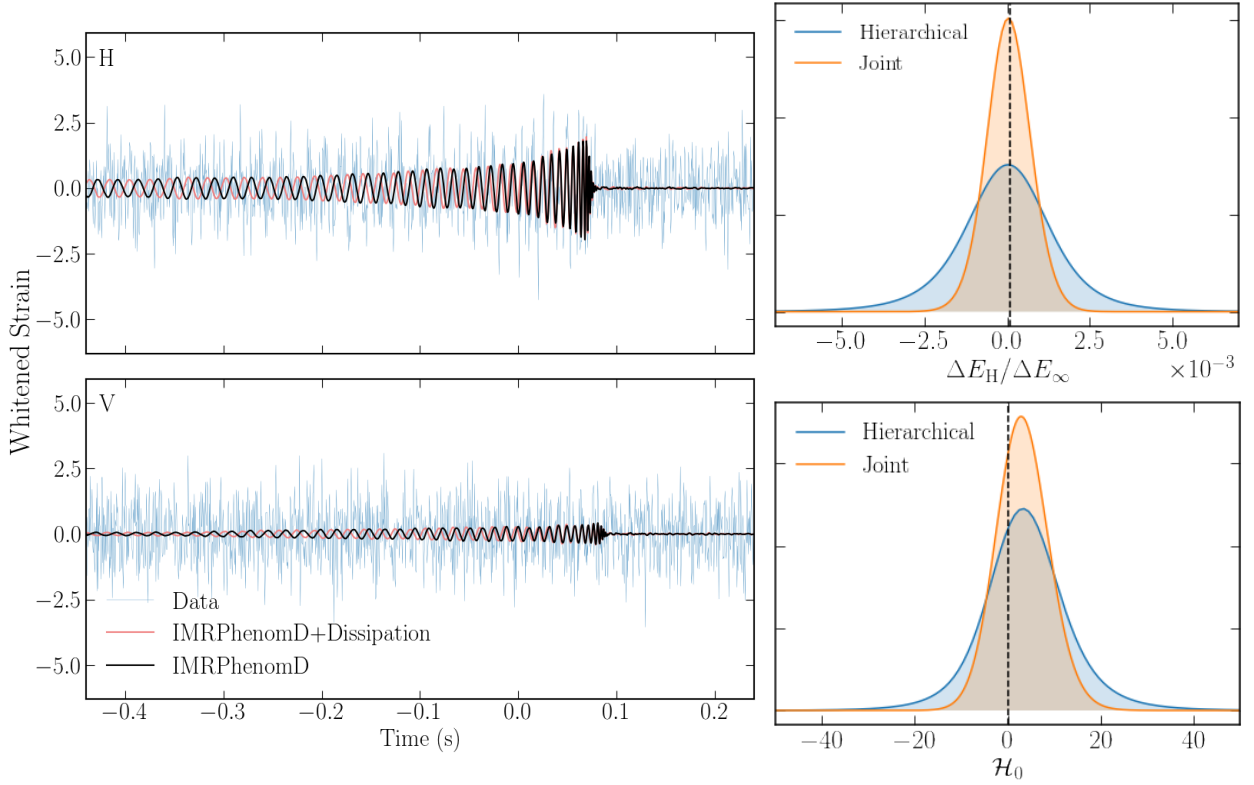


Figure 1: *Left panel:* GW strains of the IMRPhenomD and IMRPhenomD+Dissipation waveforms for a GW191216.213338 event in the Hanford and Virgo data. We choose the individual dissipation parameters $H_{1\omega} = H_{2\omega} = 10$ to clearly illustrate dephasing of the waveform due to tidal heating. *Upper right panel:* Constraints on the ratio of the energy loss $\Delta E_H/\Delta E_\infty$ due to tidal dissipation relative to radiative loss at infinity. The black dashed line represents the GR prediction $\Delta E_H/\Delta E_\infty \simeq (10^{-5}, 10^{-4})$. *Lower right panel:* Constraints on the spin-independent dissipation coefficient \mathcal{H}_0 . The black dashed line shows the GR prediction for equal mass binary black holes with $\mathcal{H}_0 = 2/45$.

In Newtonian physics, a spherically symmetric isolated compact body subjected to a weak external quadrupolar tidal moment E^{ab} generates the induced quadrupole moment Q_{ab} , whose expansion in time derivatives takes the form [44, 47]:

$$Q_{ab} = -\frac{2}{3G}k_2R^5 \left[E_{ab} - \mathcal{T} \frac{d}{dt} E_{ab} + \dots \right], \quad (2.1)$$

where R is the body's radius, and G is Newton's gravitational constant. The coefficient k_2 above is a Newtonian Love number, while \mathcal{T} is the viscous time lag between the tidal field and the body's response. In the presence of viscosity, the mass transfer rate due to the absorption of gravitational radiation is given by [32, 44, 94, 96, 123, 124],

$$\frac{dm}{dt} = \frac{2}{3G}R^5k_2\mathcal{T}\dot{E}^{ab}\dot{E}_{ab}. \quad (2.2)$$

Assuming that the body is slowly spinning, one can see that viscosity also leads to the loss of the

	Physical Quantity	90% credible interval
Dissipation coefficients	\mathcal{H}_0	$-13 < \mathcal{H}_0 < 20$
	\mathcal{H}_1	$-18 < \mathcal{H}_1 < 11$
	$\overline{\mathcal{H}}_1$	$-18 < \overline{\mathcal{H}}_1 < 16$
Relative energy loss	$\Delta E_{\text{H}}/\Delta E_{\infty}$	$-0.0026 < \Delta E_{\text{H}}/\Delta E_{\infty} < 0.0025$

Table 1: Summary of the constraints on the tidal heating coefficients for the black hole population in the LIGO-Virgo O1-O3 catalog. We also provide constraints on the ratio of the energy loss to the black hole horizon due to tidal heating to the gravitational wave energy propagated towards infinity. The GR prediction is $\mathcal{H}_0 = 2/45$ for equal mass binary black holes and $\Delta E_{\text{H}}/\Delta E_{\infty} \simeq (10^{-5}, 10^{-4})$.

angular momentum J , i.e. the tidal field induces a torque [47, 123]

$$\frac{dJ}{dt} = -\frac{4}{3G} R^5 k_2 \mathcal{T} \epsilon_{abc} \dot{E}_d^a E^{db} \hat{s}^c, \quad (2.3)$$

where $\hat{s}^c = (0, 0, 1)$ is a unit vector in the spin direction. EFT allows us to generalize these concepts beyond the Newtonian limit, for a generic compact body, arbitrary spin, and in the presence of relativistic non-linearity. In the observationally relevant case of small spin, the general expression for the dissipative (i.e. odd under time reversal) part of the electric-type induced quadrupole moment in the local asymptotic rest frame is given by

$$Q^{ij} \Big|_{\text{dis.}} = m(Gm)^4 \left[(Gm) H_{\omega} \frac{D}{D\tau} E^{ij} - H_S \chi \hat{S}^{(i} E^{k|j)} \right], \quad (2.4)$$

where τ is proper time of the black hole’s worldline, $\chi = J/(Gm^2)$ is the dimensionless spin, \hat{S}^{ij} is the unit spin tensor. The free coefficient H_{ω} generalizes the viscous lag parameter, while H_S is a new coefficient that measures the absorption of mass and angular momentum due to spin. Physically, it originates from a coordinate transformation from the local rotating frame to the local asymptotic inertial rest frame. Essentially, this term captures superradiance and tidal locking. The amplitude of H_S is set by body’s angular velocity measured at infinity.

H_S and H_{ω} are the main two parameters that we constrain with the LIGO-Virgo-KAGRA data. To do so, we consistently derive the waveform modifications following from the induced quadrupole moment (2.4). H_S and H_{ω} affect the waveforms at 2.5PN and 4PN, respectively. We also study “magnetic” (parity-odd) tidal effects, which appear at a higher post-Newtonian (PN) order. In addition, we constrain a more intuitive physical quantity, the absorption of mass following from the generalized Eq. (2.2),

$$\dot{m} = m(Gm)^5 H_{\omega} \dot{E}^{ij} \dot{E}_{ij} - m(Gm)^4 H_S \chi \left(\dot{E}^{ij} E_i^k \hat{S}_{jk} \right) + \text{magnetic}. \quad (2.5)$$

In the upper right panel of Fig. 1, we present the population level constraint on the ratio between the energy lost due to tidal dissipation, ΔE_{H} , and the radiative energy at infinity, ΔE_{∞} . We establish that, at the population level, the constraint falls within the range of $-0.0026 < \Delta E_{\text{H}}/\Delta E_{\infty} < 0.0025$, with a 90% credible level, as determined through a hierarchical Bayesian approach. Note that this constraint includes the possibility of the radiation

enhancement, similar to superradiance, which corresponds to negative values of H_ω . Our result is consistent with the general relativity prediction that BBHs should lose about a $10^{-5} - 10^{-4}$ fraction of the total radiated energy to tidal dissipation. Our main constraints are summarized in Table 2.

The primary factor contributing to tidal dissipation is represented by the 4PN spin-independent dissipation parameters H_ω . At leading order, it affects the waveforms through the mass weighted combination \mathcal{H}_0 ,

$$\mathcal{H}_0 \equiv \frac{1}{M^4} (m_1^4 H_{1\omega} + m_2^4 H_{2\omega}) , \quad (2.6)$$

where $m_{1,2}$ are the component masses, $M = m_1 + m_2$, and $H_{1,2\omega}$ are individual dissipation numbers of binary components. We show the typical waveform modifications due to this parameter in the left panel of Fig. 1. In the lower right panel of Fig. 1, we display the combined posterior, with the constraint $-13 < \mathcal{H}_0 < 20$ at 90% CL.

For binaries with spinning components, the leading-order tidal heating effects first appear at 2.5PN and are quantified by the symmetric and anti-symmetric combinations

$$\mathcal{H}_1 \equiv \frac{1}{M^3} (m_1^3 H_{1S} + m_2^3 H_{2S}) , \quad \bar{\mathcal{H}}_1 \equiv \frac{1}{M^3} (m_1^3 H_{1S} - m_2^3 H_{2S}) , \quad (2.7)$$

where $H_{1,2S}$ are the linear-in-spin tidal dissipation numbers of the binary components. The physical imprints associated with \mathcal{H}_1 and $\bar{\mathcal{H}}_1$ on GW observables are linearly proportional to the symmetric and anti-symmetric combinations of the component spins. Since most of the LVK mergers have small spin, \mathcal{H}_1 and $\bar{\mathcal{H}}_1$ are somewhat less constrained than \mathcal{H}_0 , even though the effects of these parameters is nominally stronger in the PN counting. Our constraints on these parameters from the LVK data are displayed in Table 2.

We discuss other subdominant effective dissipation numbers, such as the cubic-in-spin dissipation numbers and the magnetic counterparts of (2.6) and (2.7), in Section 3. Constraints on the magnetic-type dissipation coefficients are presented in Section 4.

From the technical side, it is worth stressing that we use exclusively the inspiral phase in our analysis in order to be conservative and agnostic about the nature of black-hole like compact objects. To achieve this, we truncate both the data, denoted as d , and the waveform, h , at the so-called tapering frequency, defined as $f_{22}^{\text{tape}} = 0.35 f_{22}^{\text{peak}}$, with f_{22}^{peak} being the peak frequency. This methodology allows us not to presuppose that the signals originate from black holes, thereby making our findings potentially applicable to a broader range of exotic binary systems. In Fig. 2, we present our constraints on the dominant dissipation number, \mathcal{H}_0 , and the ratio of energy loss, $\Delta E_H/\Delta E_\infty$, for a few selected events. Our results indicate that for individual events $|\mathcal{H}_0| \lesssim 400$ and $|\Delta E_H/\Delta E_\infty| \lesssim 0.08$ within a 90% credible interval.

3 Tidal Heating Effects on Gravitational Waves: Theory

In this section, we review the description of tidal dissipative dynamics of a single rotating body from the perspective of the worldline EFT formalism [32, 94–101]. Then in §3.4, we discuss tidal dissipation in the context of binary systems and present results for the imprints of this effect on the GW phase and amplitude.

Most of the material presented in §3.1 and §3.2 is well known in the literature; we refer the reader to the original work and excellent reviews [22, 94–96, 103, 104] for further details. Our

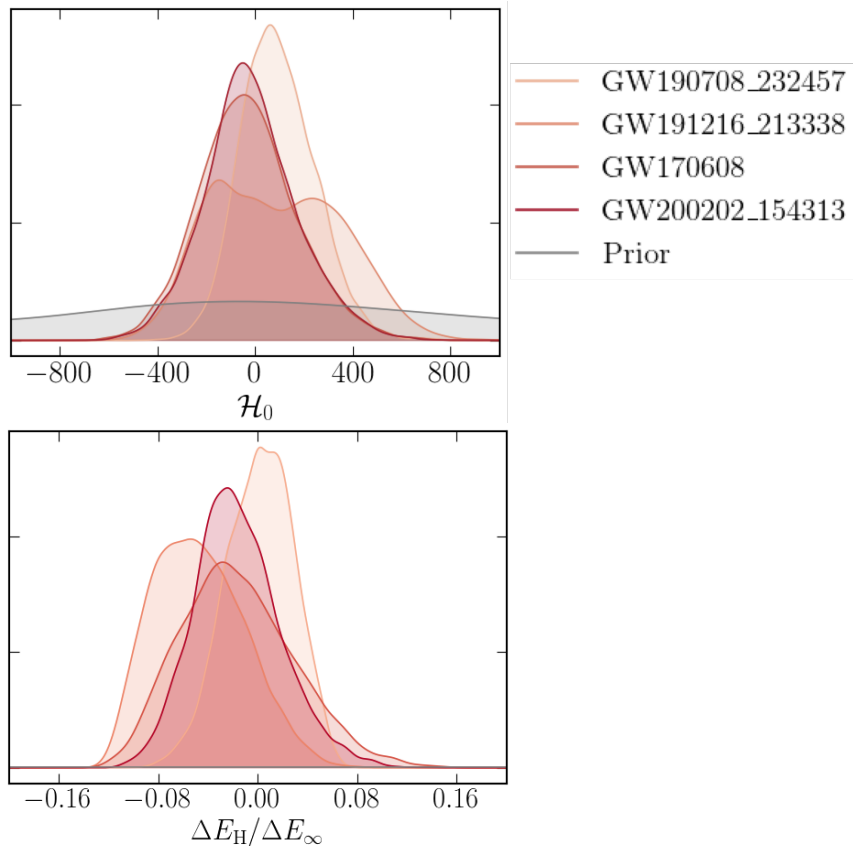


Figure 2: (*top*) Inspiral-only constraints on the dissipation number \mathcal{H}_0 for selected events. (*bottom*) Inspiral-only constraints on the ratio of the energy loss $\Delta E_H/\Delta E_\infty$.

goal here is to highlight the main conceptual features of EFT that are relevant in the context of LVK data analysis. In particular, we would like to point out that EFT makes manifest the connection between terms that appear in the LVK waveforms and the on-shell amplitudes for gravitational scattering computed in [22, 94–96, 125, 126].

3.1 Worldline EFT for Tidal Heating of a Non-Rotating Body

In worldline EFT, compact bodies are described, at leading order, as point particles. In the simplest example of a body without spin, the leading order EFT action for a single body is given by

$$S^{(0)} = -m \int ds, \quad (3.1)$$

where m is body’s mass and s is the worldline parameter which we will often choose to be equal to body’s proper time τ . In addition to action (3.1) one should consider the perturbative general relativity action for “bulk gravity,”

$$S_{\text{GR}} = - \int d^4x \sqrt{g} \frac{R}{16\pi G}. \quad (3.2)$$

Conservative dynamical effects beyond the point particle approximation, such as tidal deformations, are described by higher order operators coupled to the worldline,

$$S^{(2)} = mR^4 \int ds (c_E E^{\mu\nu} E_{\mu\nu} + c_B B^{\mu\nu} B_{\mu\nu}) + \dots, \quad (3.3)$$

where we used the electric and magnetic parts of the Weyl tensor $C_{\mu\nu\alpha\beta}$,

$$E_{\mu\nu} = C_{\mu\rho\nu\sigma} u^\rho u^\sigma, \quad B_{\mu\nu} = \frac{1}{2} \varepsilon_{\mu\rho\alpha\beta} C^{\alpha\beta}{}_{\nu\sigma} u^\rho u^\sigma, \quad (3.4)$$

u^μ is the four-velocity of the point particle. Parameters $c_{E,B}$ are dimensionless EFT Wilson coefficients (counterterms), which provide a gauge invariant definition for the static Love numbers. Note that the formal expansion parameter in worldline EFT for compact bodies is $\omega R \ll 1$, i.e. it is applicable only to describe dynamics on scales much larger than the size of the compact body, which is appropriate for the binary dynamics where ω can be associated with the orbital frequency. In what follows, in the context of non-rotating bodies, it will be convenient to work with tetrads e_μ^a defining an orthonormal frame, which satisfy

$$\eta_{ab} e_\mu^a e_\nu^b = g_{\mu\nu}(x), \quad g_{\mu\nu}(x) e_a^\mu e_b^\nu = \eta_{ab}. \quad (3.5)$$

In the body's rest frame, these tetrads reduce to

$$e_a^\mu = \delta_a^\mu, \quad (3.6)$$

where $a = 0, 1, 2, 3$ denote local Lorentz indices. In order to describe dissipative effects, one has to introduce composite multipole moments Q_{ab} that are coupled to the external gravitational field [94, 96],

$$S = - \int ds Q_{ab}^E E^{ab} - \int ds Q_{ab}^B B^{ab}. \quad (3.7)$$

The explicit form of the multipole moments $Q_{ab}^{E/B}$ is unknown. Classical physical observables depend only on their retarded Green's functions. (See Refs. [127–129] for the treatment of quantum effects.) These can be matched from gauge-invariant observables such as the cross-section for the compact body to absorb gravitons. For instance, a leading order EFT calculation gives [94]

$$\sigma_{\text{abs}}(\omega) = G\pi\omega^3 \varepsilon_{ab}^* \varepsilon_{cd} \langle Q_E^{ab} Q_E^{cd} \rangle(\omega) + \text{magnetic}, \quad (3.8)$$

where $\langle Q_E^{ab} Q_E^{cd} \rangle$ is the Wightman correlator. The underlying spherical symmetry of the unperturbed compact body dictates that

$$\langle Q_{ab}^E Q_{cd}^E \rangle(\omega) \equiv \int ds e^{i\omega s} \langle Q_{ab}^E(s) Q_{cd}^E(0) \rangle = \frac{1}{2} \left(\eta_{ac}^\perp \eta_{bd}^\perp + \eta_{ab}^\perp \eta_{cd}^\perp - \frac{2}{3} \eta_{ab}^\perp \eta_{cd}^\perp \right) F_E(\omega) \equiv \mathcal{P}_{ab,cd}^{(0)} F_E(\omega), \quad (3.9)$$

for some scalar function $F_E(\omega)$ (and the same for B), where $\eta_{ab}^\perp = \eta_{ab} - u_a u_b$ is the metric in the compact body's frame. Comparing above with the cross-section calculated in GR allows one to determine the functional form of $F_{E/B}(\omega)$. For instance, matching to the graviton absorption cross-section in black hole perturbation theory one obtains [94]

$$F_E(\omega) = F_B(\omega) = \Theta_H(\omega) \frac{2r_s^6 \omega}{45G}, \quad (3.10)$$

where $\Theta_H(\omega)$ denotes the Heaviside step function. After matching, this expression can be used to make further prediction for other observables. In the context of gravitational wave astronomy, one is interested in the expectation values $\langle Q_{ab}^{E/B} \rangle$ over the ensemble of small-scale fluctuations produced by the internal degrees of freedom of a compact body. In this case, for the adiabatic phase of the inspiral, one can assume that the external gravitational fields are weak, and apply linear response theory, yielding

$$\langle Q_{ab}^E \rangle = \int ds' G_{ab,cd}^{\text{ret}}(s-s') E^{cd}(x(s')), \quad (3.11)$$

and the same for Q_{ab}^B . Note that $E^{cd}(x(s'))$ above is the external tidal field evaluated on the compact body's worldline. The Green's function above cannot be calculated in general. Its local part is indistinguishable from the contributions from the local counterterms in $S^{(2)}$. The non-local contribution, however, is calculable, and can be expressed through the correlators that we have matched before from the absorption cross-section, yielding e.g. for the electric part [96]

$$\langle Q_{ab}^E \rangle = \frac{4r_s^2(Gm)^4}{45G} \mathcal{P}_{ab,cd}^{(0)} \frac{d}{ds} E^{cd}(x(\tau)) = \frac{4r_s^2(Gm)^4}{45G} \frac{d}{ds} E^{ab}(x(\tau)). \quad (3.12)$$

In the first approximation, i.e. neglecting interactions of the internal multipoles with ‘‘bulk’’ gravitons, EFT gives the same result as the classical linear response theory post-Newtonian adiabatic expansion over time derivatives,

$$\langle Q_{ab}^E \rangle = m(Gm)^4 \left[c_0 E_{ab} + (Gm)h_0 \frac{d}{d\tau} E^{ab} + \dots \right], \quad (3.13)$$

where we inserted m and G in order to make the coefficients c_0 and h_0 dimensionless. In the traditional post-Newtonian context, c_0 is interpreted as a static Love number. In EFT, at first order, physical observables depend on the combination of c_0 and the local counterterms in $S^{(2)}$.

We stress that strictly speaking, Eq. (3.13) is true only at the zeroth order in the interaction with bulk gravitons. In general, tail effects make the relationship between Q_{ab} and E_{ab} non-local. In the context of linear response theory, this can be heuristically interpreted as a running of dissipation coefficients. In the strict mathematical sense, within EFT, this corresponds to the renormalization of the two-point function of Q_{ab} due to its dressing with graviton loops [125, 130].

For a general body, the leading order tidal heating effect is captured by a single parameter h_0 . In the particular example of a black hole, matching of the absorption cross-sections yield

$$h_0 = \frac{4r_s^2}{45G^2m^2} = \frac{16}{45}. \quad (3.14)$$

To calculate non-conservative effects on the binary dynamics one has to introduce a composite momentum operator p_a and conveniently rewrite the point particle action as

$$S^{(0)} = - \int dx^\mu e_\mu^a p_a + \int ds (p_a p^a - m^2). \quad (3.15)$$

In the body's rest frame this action takes to usual form of the point particle action. Varying $S^{(0)}$ and $S^{(2)}$ w.r.t. x^μ one obtains, in Fermi normal coordinates [96],

$$\frac{Dp^\mu}{Ds} = e_\rho^a e_\sigma^b [\langle Q_{ab}^E \rangle \nabla^\mu E^{\rho\sigma} + \langle Q_{ab}^B \rangle \nabla^\mu B^{\rho\sigma}], \quad (3.16)$$

where $p^\mu = p^a e_a^\mu$. Multiplying this by p^μ we arrive at the final equation for the mass dynamics

$$\frac{dm^2}{ds} = 2e_\rho^a e_\sigma^b [\langle Q_{ab}^E \rangle p_\mu \nabla^\mu E^{\rho\sigma} + \langle Q_{ab}^B \rangle p_\mu \nabla^\mu B^{\rho\sigma}]. \quad (3.17)$$

If the response is purely conservative, $\langle Q_{ab} \rangle \propto E_{ab}$, the above equation integrates to a trivial solution. The dissipative part of the response at the leading order gives

$$\frac{dm^2}{ds} = 2(Gm)^5 m^2 h_0 [\dot{E}_{\rho\sigma}^2 + \dot{B}_{\rho\sigma}^2]. \quad (3.18)$$

This equation can be used now to calculate fluxes relevant for gravitational waveforms. For black holes, the result is [94]

$$\frac{dm}{ds} = \frac{16(mG)^5 m}{45} [\dot{E}_{\rho\sigma}^2 + \dot{B}_{\rho\sigma}^2]. \quad (3.19)$$

which precisely matches the classical general relativity result for the absorption of mass by a black hole in the adiabatic regime [124]. Eq. (3.18) will be used as input in gravitational waveform calculations below.

3.2 Tidal Heating of a Rotating Compact Body

The extension of the worldline EFT approach to spinning bodies is as follows. First, one writes down an effective action for a point particle with spin,

$$S^{(0)} = - \int dx^\mu e_\mu^a p_a + \int ds (p_a p^a - m^2) + \frac{1}{2} \int d\lambda S^{ab} \Omega_{ab} + \int ds l_a S^{ab} p_b, \quad (3.20)$$

with $ds = d\lambda e(\lambda)$, and λ denotes a worldline's affine parameter. The action (3.20) defines the spin tensor S_{ab} as a canonical conjugate of the angular velocity. l_a in the rightmost above term is the Lagrange multiplier that eliminates spurious degrees of freedom in S_{ab} . As before, p_a and S_{ab} are treated as composite operators that depend on unspecified internal dynamics of the compact body. It will be convenient to define tetrads that describe a co-rotating frame, $e_a^0 = \delta_a^0$ and

$$e_a^i = \begin{bmatrix} \cos(\Omega x^0) & -\sin(\Omega x^0) & 0 \\ \sin(\Omega x^0) & \cos(\Omega x^0) & 0 \\ 0 & 0 & 1 \end{bmatrix}, \quad (3.21)$$

where Ω is body's angular velocity. The angular velocity tensor reads

$$\Omega_{ab} \equiv -g_{\mu\nu} e_a^\mu \frac{D}{Ds} e_b^\nu = -\Omega_{ba} \quad (3.22)$$

Action (3.20) generates the usual Papapetrou-Mathison equations on p_μ and $S_{\mu\nu}$ for a point particle. In order to describe finite-size effects, we must supplement action (3.20) with the finite-size action (3.7). The generalized Papapetrou-Mathison equations for mass and spin dynamics then read [96]

$$\begin{aligned} \frac{dm^2}{ds} &= 2e_\rho^a e_\sigma^b [\langle Q_{ab}^E \rangle p_\mu \nabla^\mu E^{\rho\sigma} + \langle Q_{ab}^B \rangle p_\mu \nabla^\mu B^{\rho\sigma}], \\ \frac{dS^2}{ds} &= \langle Q_{ab}^E \rangle E^{bc} S_c^a + \langle Q_{ab}^B \rangle B^{bc} S_c^a, \end{aligned} \quad (3.23)$$

where $S^2 = \frac{1}{2}S^{\mu\nu}S_{\mu\nu}$. Note that the derivatives w.r.t. s include both the intrinsic time-dependence of the body as well as the co-rotation, i.e.

$$\frac{D}{Ds}E^{ab} = e_\mu^a e_\nu^b \frac{D}{Ds}E^{\mu\nu} + \Omega^a{}_c E^{cb} + \Omega^b{}_c E^{ca}. \quad (3.24)$$

In order to extract the two-point functions of $Q_{ab}^{E,B}$ one can first use symmetry arguments to decompose $\langle Q_{ab}^{E,B} Q_{cd}^{E,B} \rangle$ over SO(3) STF tensors with different azimuthal numbers m_ℓ ,

$$\langle Q_{ab}^{E/B} Q_{cd}^{E/B} \rangle = \sum_{i=0}^4 A_i^{E/B}(s-s') \mathcal{P}_{ab,cd}^{(i)}, \quad (3.25)$$

where the projection tensors $\mathcal{P}_{ab,cd}^{(i)}$ can be found in [96]. Then one can calculate the probability for a compact body to absorb a graviton in the EFT, yielding

$$p(1 \rightarrow 0) = \frac{4G\omega^5}{5} \sum_{i=0}^4 m_\ell^i (A_i^E(\omega - m\Omega) + A_i^B(\omega - m\Omega)), \quad (3.26)$$

and match it to general relativity results [62, 63]. For instance, for black holes one can obtain

$$\begin{aligned} A_0^{E/B}(\omega) &= \frac{16(r_+^2 + a^2)}{45G} (Gm)^4 (1 - \chi^2)^2 \Theta_H(\omega)\omega \equiv h_0 \Theta_H(\omega)\omega, \\ A_2^{E/B}(\omega) &= \frac{2(r_+^2 + a^2)}{9G} (Gm)^4 \chi^2 (1 - \chi^2) \Theta_H(\omega)\omega \equiv h_2 \Theta_H(\omega)\omega, \\ A_4^{E/B}(\omega) &= \frac{8(r_+^2 + a^2)}{45G} (Gm)^4 \chi^4 \Theta_H(\omega)\omega \equiv h_4 \Theta_H(\omega)\omega, \end{aligned} \quad (3.27)$$

and $A_1^{E/B} = A_3^{E/B} = 0$, where we used $\chi = a/(Gm)$ and $r_+ = M + \sqrt{M^2 + a^2}$ is the outer horizon of a rotating black hole. We see that $A_i^{E/B}/\omega$ is constant for physical positive frequencies. Importantly, with our choice of tetrads, the superradiance effect is captured automatically. The superradiance appears naturally in the EFT approach as a result of a coordinate transformation from a body's rest frame where the correlators of $Q_{ab}^{E/B}$ are defined, to local static frame of the asymptotic observer where the measurements are done. Matching EFT and black hole perturbation theory absorption cross-sections we obtain

$$\Omega = \Omega_H = \frac{a}{r_+^2 + a^2}. \quad (3.28)$$

Using the Wightman two point functions of composite multipoles, one can compute the non-local part of retarded Green's function and obtain

$$\langle Q_{ab}^E(s) \rangle \Big|_{\text{non-local}} = \sum_{i=0}^4 h_i \mathcal{P}_{ab,cd}^{(i)} \frac{d}{ds} E^{cd}, \quad (3.29)$$

with $h_1 = h_3 = 0$, and an analogous expression for the magnetic response. We note, again, that at the leading order, the EFT expansion for the two-point function reproduces the classical expression for the linear response of the quadrupole moments,

$$\begin{aligned}
\langle Q_{ab}^E \rangle &= -m(Gm)^4 \left[(\lambda^E)_{abcd} E^{cd} - (Gm)(\lambda_\omega^E)_{abcd} \frac{D}{Ds} E^{cd} + \dots \right], \\
\langle Q_{ab}^B \rangle &= -m(Gm)^4 \left[(\lambda^B)_{abcd} B^{cd} - (Gm)(\lambda_\omega^B)_{abcd} \frac{D}{Ds} B^{cd} + \dots \right],
\end{aligned} \tag{3.30}$$

where $(\lambda^{E/B})_{abcd}$ and $(\lambda_\omega^{E/B})_{abcd}$ are linear static and time-dependent response tensors in the body's rest frame, and dots stand for higher order time derivatives. The transformation from the local co-rotating frame to the local inertial frame is given by Eq. (3.24).

In what follows we will work within a linear response approach, which is sufficient at the leading order in the PN scheme. We will use the symmetries of the problem, parity and axial symmetry, to expand the above response tensors $(\lambda^{E/B})_{abcd}$ and $(\lambda_\omega^{E/B})_{abcd}$ over an appropriate basis of symmetric trace-free (STF) tensors. We will use spin to describe the breaking of rotational symmetry. Specifically, we will use the unit spin tensor \hat{S}_{ab} (with normalization $\hat{S}_{ab}\hat{S}^{ab} = 2$) and the Pauli-Lubanski unit spin vector, $\hat{s}^a \equiv (1/2)\epsilon^{abc}\hat{S}_{bc}$. The isomorphism between STF tensors and spherical harmonics can be used to connect tensors in our basis with the decomposition of the two-point functions of Q in harmonic space that we used before. Then, one can write the following expression for the frequency-independent part of the response:

$$(\lambda^{E/B})_{cd}^{ab} = \Lambda^{E/B} \delta_{\langle c}^{(a} \delta_{d)}^{b\rangle} + \Lambda_{S^2}^{E/B} \chi^2 \hat{s}^{\langle a} s_{\langle c} \delta_{d)}^{b\rangle} + \Lambda_{S^4}^{E/B} \chi^4 \hat{s}^{\langle a} \hat{s}_{\langle c} \hat{S}^{b\rangle} \hat{s}_{d)} \rangle, \tag{3.31}$$

where angular brackets denote the operation of symmetrization and a subsequent subtraction of traces. The three response tensors above are degenerate with the contribution of local worldline counterterms. This is because the response operators associated with tensors $\Lambda^{E/B}$, $\Lambda_{S^2}^{E/B}$, and $\Lambda_{S^4}^{E/B}$ are time-reversal even. Note that the response tensor above could include extra terms,

$$\lambda^{E/B}{}_{cd}{}^{ab} \supset \tilde{H}_S^{E/B} \chi \hat{S}_{\langle c}^{(a} \delta_{d)}^{b\rangle} + \tilde{H}_{S^3}^{E/B} \chi^3 \hat{s}^{\langle a} \hat{s}_{\langle c} \hat{S}^{b\rangle} \hat{s}_{d)} \rangle, \tag{3.32}$$

which nominally describe static dissipation due to spin in the co-rotating frame. At the level of the Wightman function, these correspond to $A_1^{E/B}$ and $A_3^{E/B}$. They are not forbidden by symmetries, but they do not have a classical interpretation in the Newtonian limit. In addition, these parameters vanish identically for black holes. Therefore, in what follows we will not consider these operators.

A similar symmetry-based decomposition can be applied to the time-dependent response tensors in

$$\begin{aligned}
(3.30): \\
(\lambda_\omega^{E/B})_{cd}^{ab} &= H_\omega^{E/B} \delta_{\langle c}^{(a} \delta_{d)}^{b\rangle} + \Lambda_{S,\omega}^{E/B} \chi \hat{S}_{\langle c}^{(a} \delta_{d)}^{b\rangle} + H_{S^2,\omega}^{E/B} \chi^2 \hat{s}^{\langle a} \hat{s}_{\langle c} \delta_{d)}^{b\rangle} \\
&\quad + \Lambda_{S^3,\omega}^{E/B} \chi^3 \hat{s}^{\langle a} \hat{s}_{\langle c} \hat{S}^{b\rangle} \hat{s}_{d)} \rangle + H_{S^4,\omega}^{E/B} \chi^4 \hat{s}^{\langle a} \hat{s}_{\langle c} \hat{S}^{b\rangle} \hat{s}_{d)} \rangle.
\end{aligned} \tag{3.33}$$

The operators with even powers of spin, associated with $H_\omega^{E/B}$, $H_{S^2,\omega}^{E/B}$, $H_{S^4,\omega}^{E/B}$, have one time derivative and hence they are odd under time reversal, i.e. they capture dissipative effects. These operators cannot be generated by a local worldline action. In contrast, the other terms above correspond to conservative time-reversal even operators, which be reproduced by local counterterms.

Let us consider now the term proportional to $H_\omega^{E/B}$ and focus, for concreteness on the electric response,

$$\langle Q_{ab}^E \rangle \Big|_{\text{non-local}} = m(Gm)^5 H_\omega^E \frac{D}{D_S} E_{ab}. \quad (3.34)$$

Using the analog of the Euler rotation equation (3.24), and switching back asymptotically flat inertial frame we obtain,

$$\langle Q_E^{ij} \rangle \Big|_{\text{non-local}} = m(Gm)^5 H_{S^0, \tilde{\omega}}^E \left[2\Omega \langle^i_k E^{k|j} \rangle + \frac{D}{D\tau} E^{ij} \right]. \quad (3.35)$$

In harmonic space, we obtain the following expression for the angular coefficients [97]

$$\langle Q_{\ell m_\ell}^E \rangle \Big|_{\text{non-local}} = -im(Gm)^5 H_\omega^E (\omega - m_\ell \Omega) E_{\ell m_\ell}, \quad (3.36)$$

where Ω is the angular velocity of rotation. We see that the square brackets in Eq. (3.35) describe the kinematic effect of superradiance encoded in the frame transformation. The EFT expansion in the co-rotating frame incorporates this phenomenon automatically.

Most of the O1-O3 LIGO-Virgo events have small spin [3, 4, 58], which suggests carrying out parameter estimation only for spin-independent and linear in spin effects. If we consider only the time-derivative operators in the co-rotating frame, we end up with three free parameters, H_ω^E, H_ω^B and Ω in the local asymptotic frame, see Eq. (3.35),

$$\langle Q_{E/B}^{ij} \rangle \Big|_{\text{non-local}} = m(Gm)^4 \left[(Gm) H_\omega^{E/B} \frac{D}{D\tau} E^{ij} - H_S^{E/B} \chi \hat{S} \langle^i_k E^{k|j} \rangle \right], \quad (3.37)$$

with $H_S^{E/B} = -2Gm\Omega\chi^{-1}H_\omega^{E/B}$. The generalized mass and spin dynamics equations following from the symmetry-based ansatz (3.33) are given by

$$\begin{aligned} \dot{m} &= m(Gm)^4 \left[(Gm) H_\omega^E \dot{E}^{ij} \dot{E}_{ij} + (Gm) H_\omega^B \dot{B}^{ij} \dot{B}_{ij} - H_S^E \chi \left(\dot{E}^{ij} E_i^k \hat{S}_{jk} \right) - H_S^B \chi \left(\dot{B}^{ij} B_i^k \hat{S}_{jk} \right) \right], \\ \dot{J} &= -m(Gm)^4 \left[-2H_S^E \chi \left(E^{ij} E_{ij} \right) + 3H_S^E \chi \left(E_i^k E_{jk} \hat{s}^i \hat{s}^j \right) + (Gm) H_\omega^E \left(\dot{E}^{ij} E_i^k \hat{S}_{jk} \right) \right. \\ &\quad \left. - 2H_S^B \chi \left(B^{ij} B_{ij} \right) + 3H_S^B \chi \left(B_i^k B_{jk} \hat{s}^i \hat{s}^j \right) + (Gm) H_\omega^B \left(\dot{B}^{ij} B_i^k \hat{S}_{jk} \right) \right]. \end{aligned} \quad (3.38)$$

where the J is the angular momentum. These equations provide input for our waveform calculations.

We note that one should consider the leading dissipation numbers H_ω^E and H_ω^B separately. However, for black holes these two parameters turns out to be the same due to the electric-magnetic duality of linear black hole perturbations, which holds for both static and spinning black holes in four dimensions [94, 95, 107, 109, 120–122]. In what follows we will consider both the general situation, and the case when our compact black-hole like objects obey the electric-magnetic duality.

Finally, let us note that §3.4, we will show that, for aligned-spin quasi-circular orbits, the spin-linear H_S^E and spin-independent H_ω^E dissipation parameters first appear in gravitational waveforms at 2.5PN and 4PN respectively.

3.3 Estimates for Tidal Dissipation Coefficients

At the microscopic level, tidal dissipation of fluid bodies is generated by viscosity [47, 49, 89], suggesting:

$$H_{\omega}^{E/B} \sim \Lambda^{E/B} \times \frac{\tau_d}{Gm}, \quad \Lambda^{E/B} \sim \left(\frac{R}{Gm} \right)^5, \quad (3.39)$$

where τ_d is the tidal lag time. In the Eulerian fluid dynamics the tidal lag time can be expressed through the kinematic viscosity ν and the star radius R ,

$$\tau_d \sim \frac{\nu R}{Gm}. \quad (3.40)$$

The kinematic viscosity for a general fluid can be estimated as $\nu \sim l_{\text{mfp}} \langle v \rangle$, where l_{mfp} is the mean free path and $\langle v \rangle \sim (k_B T / \mathcal{M})^{1/2}$ is the average velocity of fluid particles (k_B is the Boltzmann constant, T is fluid temperature, and \mathcal{M} is the particle mass). For black holes, the dissipation coefficient is given by

$$\tau_d \sim \frac{cr_s^2}{Gm}. \quad (3.41)$$

If we naively interpret this result as coming from fluid dynamics, we would conclude that the fluid has a mean free path equal to that of the size of the compact object and the mean velocity is equal to c . Obviously, this represents a very extreme scenario that is unlikely to realize in any actual microscopic model. This, however, sets a good benchmark for typical dissipation coefficients of celestial bodies. Denoting $\nu_{\text{BH}} \equiv cr_s$, we get

$$H_{\omega}^{E/B} \sim \left(\frac{R}{Gm} \right)^6 \times \left(\frac{\nu}{\nu_{\text{BH}}} \right), \quad (3.42)$$

For usual stars, the mean free path of the ionized gas is $l_{\text{mfp}} \sim \frac{k_B^2 T^2}{\pi e^4 n} \sim 10^{-3} \text{cm}$, which gives $\nu \sim 10^3 \text{cm}^2 \text{sec}^{-1}$, resulting in the following estimate:

$$\text{Usual stars: } \nu / \nu_{\text{BH}} \sim 10^{-13}, \quad (3.43)$$

where we used $T = 10^4 \text{K}$, $n \sim 10^{16} \text{cm}^{-3}$, $m = 1m_{\odot}$. For neutron stars, the highest realistic value of the bulk viscosity is $\zeta \sim 10^{30} \text{g/cm/s}$ [131–134]. For typical densities of 10^{15}g/cm^3 this implies

$$\text{Neutron stars: } \nu / \nu_{\text{BH}} \sim 0.1, \quad (3.44)$$

where we assumed $m = 1.5 m_{\odot}$. Owing to the extra enhancement by $(R/r_s)^6 \sim 5^6 \simeq 10^4$, we see that the dissipation coefficient of neutron stars may be non-negligible.

The dissipation parameters of Kerr black holes can be read off from black hole perturbation theory calculations [94, 100, 108, 109, 135]:

$$H_{\omega}^{E/B} = \frac{8}{45} \left(1 + \sqrt{1 - \chi^2} \right), \quad H_S^{E/B} = -\frac{8}{45} (1 + 3\chi^2). \quad (3.45)$$

In the observationally relevant small spin limit we have:

$$H_{\omega}^{E/B}(\chi \rightarrow 0) = \frac{16}{45}, \quad H_S^{E/B}(\chi \rightarrow 0) = -\frac{8}{45}. \quad (3.46)$$

The relationship between $H_S^{E/B}$ and $H_\omega^{E/B}$ follows from superradiance. This relationship is more complex for a general body, where $H_S^{E/B}$ depend on the body's angular velocity (measured at infinity), implying

$$H_S^{E/B} = -2 \frac{Gm\Omega}{\chi} H_\omega. \quad (3.47)$$

Since the angular velocity in general is not determined by spin [136], we could not deduce $H_S^{E/B}$ entirely from H_ω . For Kerr black holes, however, one can use relations $\Omega^{ab} = \Omega \hat{S}^{ab}$, $\Omega = a/(r_+^2 + a^2)$, implying

$$H_S^{E/B}|_{\text{Kerr}} = -\frac{1}{2} H_\omega^{E/B}|_{\text{Kerr}}, \quad (3.48)$$

which we have already seen in Eq. (3.46). Simulations of rotating quark stars in [137, 138] suggest that

$$\Omega \approx \text{const} \times \frac{J}{Gm^2} \left(\frac{Gm}{R^3} \right)^{1/2}, \quad \Rightarrow \quad \frac{H_S}{H_\omega} \sim \left(\frac{r_s}{R} \right)^{3/2} \lesssim 1, \quad (3.49)$$

i.e. the dissipation coefficients associated with angular velocity should be somewhat suppressed w.r.t. the spin-independent dissipation numbers H_ω .

3.4 Tidal Heating Imprints on Waveforms

In Fourier space, the gravitational waveform for a quasi-circular aligned-spin binary system in the (2, 2) radiation mode takes the general form

$$\tilde{h}(f) = A(f) e^{-i\psi(f)}, \quad \tilde{h}_+(f) = \tilde{h}(f) \frac{1 + \cos^2 \iota}{2}, \quad \tilde{h}_\times(f) = -i\tilde{h}(f) \cos \iota \quad (3.50)$$

where A is the amplitude, ψ is the phase, $h_{+,\times}$ are the plus and cross GW polarizations, and ι is the inclination angle between the line of sight and the orbital angular momentum.² We will derive now contributions from tidal dissipation in ψ and A relevant for the inspiral part of the waveform. We will present results for a general waveform that are applicable for any general compact objects, and a reduced waveform that is useful for black hole binary tests. The latter are simplified by using the electric-magnetic duality and optionally the superradiance relation if we assume the black holes have small spins.

Let us start with the impact of tidal heating on a general compact body. We consider the inspiral part of the gravitational waveform, where the imprints on observables can be derived analytically. Our derivation here will contain only the main results. Details of the intermediate calculations can be found in Appendix A. We start with the energy balance equation

$$-\mathcal{F}_\infty - \dot{M} = \dot{\mathcal{E}}, \quad (3.51)$$

where \mathcal{E} is the binding energy, \mathcal{F}_∞ is the energy flux radiated to infinity, $M = m_1 + m_2$ is the total mass, $\dot{M} = \dot{m}_1 + \dot{m}_2$ is the total tidal heating flux absorbed by both binary components, and the overdot stands for a time derivative. For an aligned spin quasi-circular orbit, the energy flux absorbed by the component mass m_1 is (see Appendix A)

²In principle, the functional form of ι in $h_{+,\times}$ shown in (3.50) only applies when A contains only the leading order amplitude – additional angular dependences in ι would appear when higher order PN corrections to A are taken into account, see e.g. [139–141]. However, in practice we found incorporating PN corrections in the amplitude leads to very little or even no changes to parameter estimation results, and we ignore these detailed angular dependences for simplicity.

$$\begin{aligned} \dot{m}_1(v) = & \left(\frac{9H_{1S}^E m_1^3 \eta^2 \chi_1}{M^3} \right) v^{15} + \left(-\frac{9H_{1S}^E m_1^3 (-2M - m_1 + 3M\eta) \eta^2 \chi_1}{M^4} \right. \\ & \left. + \frac{9H_{1S}^B m_1^3 \eta^2 \chi_1}{M^3} \right) v^{17} + \left(\frac{18H_{1\omega} m_1^4 \eta^2}{M^4} \right) v^{18} , \end{aligned} \quad (3.52)$$

where $v = (\pi M f)^{1/3}$ is the PN velocity and $\eta \equiv m_1 m_2 / M^2$ is the symmetric mass ratio. The expression for \dot{m}_2 is obtained by interchanging the $1 \leftrightarrow 2$ indices in Eq. (3.52). Compared to the leading order Einstein quadrupolar flux, $\mathcal{F}_\infty^{\text{LO}} = 32\eta^2 v^{10}/5$, Eq. (3.52) shows that the leading tidal heating effect contributes at 2.5PN order.

In the stationary phase approximation [142], the phase can be derived by iteratively solving for the orbital phase $\phi(v)$ and time $t(v)$, both of which depend on \dot{v} [143, 144]. The \dot{v} term can be obtained by applying the chain rule on $\dot{\mathcal{E}}$

$$\dot{\mathcal{E}} = \frac{\partial \mathcal{E}}{\partial v} \dot{v} + \frac{\partial \mathcal{E}}{\partial m_1} \dot{m}_1 + \frac{\partial \mathcal{E}}{\partial m_2} \dot{m}_2 , \quad (3.53)$$

where we extended the chain rule to the component masses as well.³ The terms which depend on $\dot{m}_{1,2}$ in (3.53) are sometimes referred to as ‘‘secular change in mass’’ and provide additional tidal heating contributions to the phase beyond the component flux (3.52). In particular, since $\partial \mathcal{E} / \partial m \propto v^2$, these terms start contributing to the phase at 3.5PN order [145]. The resulting TaylorF2 phase reads

$$\psi(v) = 2\pi f t_0 - \phi_0 - \frac{\pi}{4} + \frac{3}{128\eta v^5} \left[\psi^{\text{PP}}(v) + \psi^{\text{TDN}}(v) \right] , \quad (3.54)$$

where t_0 and ϕ_0 are the time and phase of coalescence, $\psi^{\text{PP}}(v) = 1 + \dots$ is the point particle contribution which we retain up to 4PN order for the non-spinning terms and up to 3.5PN order for the aligned-spin terms [18, 146]; we list these coefficients in (A.21). The phase contributions from the tidal dissipation numbers are (see Appendix A)

$$\psi^{\text{TDN}}(v) = \underbrace{v^5(1 + 3 \ln v) \psi_{2.5\text{PN}}^{\text{TDN}}}_{\text{linear spin}} + \underbrace{v^7 \psi_{3.5\text{PN}}^{\text{TDN}}}_{\text{linear} + \dots} + \underbrace{v^8(1 - 3 \ln v) \psi_{4\text{PN}}^{\text{TDN}}}_{\text{spin independent} + \dots} , \quad (3.55)$$

where the spin dependent terms are retained up to 3.5PN order while the spin-independent phase starts appearing at 4PN order. Note that here we focus only on the contributions up to linear order in spin; we drop the spin-quadratic, spin cubic and spin quartic terms. In this approximation we have:

$$\begin{aligned} \psi_{2.5\text{PN}}^{\text{TDN}} &= \left(\frac{25}{4} \mathcal{H}_1^E \chi_s + \frac{25}{4} \bar{\mathcal{H}}_1^E \chi_a \right) , \\ \psi_{3.5\text{PN}}^{\text{TDN}} &= \left(\frac{225}{8} \mathcal{H}_1^B + \frac{102975}{448} \mathcal{H}_1^E + \frac{675}{32} \bar{\mathcal{H}}_1^E \delta + \frac{1425}{16} \mathcal{H}_1^E \eta \right) \chi_s \\ &\quad + \left(\frac{225}{8} \bar{\mathcal{H}}_1^B + \frac{102975}{448} \bar{\mathcal{H}}_1^E + \frac{675}{32} \mathcal{H}_1^E \delta + \frac{1425}{16} \bar{\mathcal{H}}_1^E \eta \right) \chi_a \\ \psi_{4\text{PN}}^{\text{TDN}} &= \frac{25}{2} \mathcal{H}_0^E + \text{other spin-dependent terms} , \end{aligned} \quad (3.56)$$

³The chain rule could in principle be extended to other intrinsic variables, for instance the component spins which leads to additional terms such as $\dot{\mathcal{E}} \supset (\partial \mathcal{E} / \partial \chi_i) \dot{\chi}_i, i = 1, 2$. However, these terms appear beyond 3.5PN order in the phase and are therefore neglected in this work.

Effective Dissipation Numbers	PN Orders for General Orbits	PN Orders for Aligned-Spin Quasi-Circular Orbits
$\mathcal{H}_1^E, \overline{\mathcal{H}}_1^E$	2.5PN, 3.5PN, ...	2.5PN, 3.5PN, ...
$\mathcal{H}_1^B, \overline{\mathcal{H}}_1^B$	3.5PN, ...	3.5PN, ...
\mathcal{H}_0^E	4PN, ...	4PN, ...
\mathcal{H}_0^B	5PN, ...	5PN, ...

Table 2: Summary of the PN orders at which the effective dissipation numbers (3.57) appear in waveform observables, for both general orbits and for aligned-spin quasi-circular orbits. In this work, we retain the spin-dependent terms up to 3.5PN order and the spin-independent term up to 4PN order.

where $\delta = (m_1 - m_2)/M$ and $\eta = m_1 m_2 / M^2$. In (3.56) we introduced several effective mass-weighted tidal dissipation numbers

$$\begin{aligned} \mathcal{H}_1^{E/B} &\equiv \frac{1}{M^3} \left(m_1^3 H_{1S}^{E/B} + m_2^3 H_{2S}^{E/B} \right), & \overline{\mathcal{H}}_1^{E/B} &\equiv \frac{1}{M^3} \left(m_1^3 H_{1S}^{E/B} - m_2^3 H_{2S}^{E/B} \right), \\ \mathcal{H}_0^{E/B} &\equiv \frac{1}{M^4} \left(m_1^4 H_{1\omega}^{E/B} + m_2^4 H_{2\omega}^{E/B} \right), \end{aligned} \quad (3.57)$$

which are better measured than the individual component dissipation numbers in data. Note that the spin-dependent terms consist of both symmetric and antisymmetric counterparts, which are labeled without and with an overline respectively. The subscripts 1 and 0 denote the linear-in-spin dependence, cubic-in-spin dependence and spin-independence of those coefficients respectively. For the spin-independent cases, the component dissipation numbers would combine to form a single effective dissipation number (this is analogous to the leading spin-independent effective Love number, which is often denoted as $\tilde{\Lambda}$ in the literature [33]). Substituting the black hole values (3.45) into (3.56), we are able to reproduce known results for the BBH waveform phase, which is known up to 3.5PN order [145].

We summarize the PN orders at which the effective dissipation numbers affect waveforms for general orbits and for aligned-spin quasi-circular orbits in Table 2. This table illustrates several interesting patterns in the PN counting that are worth highlighting. Firstly, due to the relative velocity suppression between the magnetic and electric tidal fields $B_{\ell m_\ell} \sim v E_{\ell m_\ell}$, Eq. (3.30) dictates that all magnetic tidal dissipation effects first appear at 1PN order higher than their electric counterparts. Furthermore, due to the fact that $M\omega \sim v^3$, the spin-independent terms $\mathcal{H}_0^{E/B}$ are 1.5PN suppressed compared to the linear-spin counterparts $\mathcal{H}_1^{E/B}, \overline{\mathcal{H}}_1^{E/B}$.

It is important to keep in mind that $\mathcal{H}_1^{E/B}$ are negative definite due to superradiance. Physically, this negative sign can be interpreted as the energy extraction process increasing the binding energy of the binary, which widens the orbit and leads to a smaller orbital velocity. On the other hand, $\mathcal{H}_0^{E/B}$ are positive definite because they represent energy absorption. Finally, the asymmetric effective dissipation numbers $\overline{\mathcal{H}}_1^{E/B}$ can be either positive or negative, depending on the relative sizes of the mass weighting and the dissipation numbers of the binary components.

For completeness, we also computed the imprints of tidal dissipation on the GW amplitude. Similar to the phase (3.54), the total amplitude can be separated into the point-particle terms

and the tidal heating terms

$$A(f) = \sqrt{\frac{5}{24}} \frac{\mathcal{M}^{5/6}}{D\pi^{2/3}} f^{-7/6} \left[A^{\text{PP}}(f) + A^{\text{TDN}}(f) \right], \quad (3.58)$$

where \mathcal{M} is the chirp mass and D is the luminosity distance. The point particle terms are shown in (A.31) while tidal dissipation contributes in the following manner

$$A^{\text{TDN}}(f) = v^5 A_{2.5\text{PN}}^{\text{TDN}} + v^7 A_{3.5\text{PN}}^{\text{TDN}} + v^8 A_{4\text{PN}}^{\text{TDN}}, \quad (3.59)$$

with the PN coefficients

$$\begin{aligned} A_{2.5\text{PN}}^{\text{TDN}} &= -\frac{45}{64} \mathcal{H}_1^E \chi_s - \frac{45}{64} \bar{\mathcal{H}}_1^E \chi_a, \\ A_{3.5\text{PN}}^{\text{TDN}} &= -\left(\frac{45}{64} \bar{\mathcal{H}}_1^B + \frac{73755}{14336} \bar{\mathcal{H}}_1^E + \frac{45}{128} \mathcal{H}_1^E \delta + \frac{465}{512} \bar{\mathcal{H}}_1^E \eta \right) \chi_a \\ &\quad + \left(-\frac{45}{64} \mathcal{H}_1^B - \frac{73755}{14336} \mathcal{H}_1^E - \frac{45}{128} \bar{\mathcal{H}}_1^E \delta - \frac{465}{512} \mathcal{H}_1^E \eta \right) \chi_s, \\ A_{4\text{PN}}^{\text{TDN}} &= -\frac{45}{32} \mathcal{H}_0^E. \end{aligned} \quad (3.60)$$

In practice, we find that incorporating these corrections to the waveform amplitude yield marginal to no changes to the parameter estimation results for the O1-O3 events (see also Footnote 2).

3.5 Simplified Waveforms for Binary Black Holes

So far, we have worked without assumptions on the nature of the compact object. However, several simplifications to the waveform can be made if we restrict ourselves to binary black holes (BBH) and intend to constrain the dissipation parameters of black holes (3.45). To this end, we can exploit the electric-magnetic duality to reduce number of parameters in Eq. (3.56). Setting the electric and magnetic dissipation coefficients to the same values, $\mathcal{H}^B = \mathcal{H}^E$, $\bar{\mathcal{H}}^B = \bar{\mathcal{H}}^E$, we reduce the set of seven tidal dissipation numbers in (3.56) to five parameters:

$$\begin{aligned} \text{E/B Duality for black holes: } \quad &\mathcal{H}^B = \mathcal{H}^E, \quad \bar{\mathcal{H}}^B = \bar{\mathcal{H}}^E \\ &\{\mathcal{H}_1^E, \bar{\mathcal{H}}_1^E, \mathcal{H}_1^B, \bar{\mathcal{H}}_1^B, \mathcal{H}_0^E\} \rightarrow \{\mathcal{H}_1, \bar{\mathcal{H}}_1, \mathcal{H}_0\}. \end{aligned} \quad (3.61)$$

In this case we drop the E/B superscripts for brevity. For future convenience, we will duplicate the tidal dissipation phases below but with the 3.5PN linear-spin term now simplified:

$$\begin{aligned} \psi_{2.5\text{PN}}^{\text{TDN}} &= \left(\frac{25}{4} \mathcal{H}_1 \chi_s + \frac{25}{4} \bar{\mathcal{H}}_1 \chi_a \right), \\ \psi_{3.5\text{PN}}^{\text{TDN}} &= \left(\frac{115575}{448} \mathcal{H}_1 + \frac{675}{32} \bar{\mathcal{H}}_1 \delta + \frac{1425}{16} \mathcal{H}_1 \eta \right) \chi_s \\ &\quad + \left(\frac{115575}{448} \bar{\mathcal{H}}_1 + \frac{675}{32} \mathcal{H}_1 \delta + \frac{1425}{16} \bar{\mathcal{H}}_1 \eta \right) \chi_a, \\ \psi_{4\text{PN}}^{\text{TDN}} &= \frac{25}{2} \mathcal{H}_0 + \text{other spin-dependent terms}. \end{aligned} \quad (3.62)$$

One could further use the superradiance condition for black holes (3.48), which relates the linear-in-spin and spin-independent dissipation numbers, such that

$$\mathcal{H}_1 \approx -\frac{1}{2M^3} (m_1^3 H_{1\omega} + m_2^3 H_{2\omega}), \quad \bar{\mathcal{H}}_1 \approx -\frac{1}{2M^3} (m_1^3 H_{1\omega} - m_2^3 H_{2\omega}). \quad (3.63)$$

Notice that due to different mass scaling in \mathcal{H}_1 and \mathcal{H}_0 they are not equal to each other in this approximation,

$$\text{Small-Spin Black Hole Superradiance: } \{\mathcal{H}_1, \overline{\mathcal{H}}_1, \mathcal{H}_0\} \rightarrow \{\mathcal{H}_1, \overline{\mathcal{H}}_1\}. \quad (3.64)$$

This assumption simplifies parameter estimation even further, reducing the set of independent tidal dissipation parameters to only two.

4 Constraints on Tidal Heating from LVK O1-O3 Data

In this section, we present the parameter estimation (PE) results for the tidal dissipation parameters. We will separate our discussion into two subsections: one that incorporates the tidal dissipation phase contributions (3.56) to IMRPhenomD [147], an inspiral-merger-ringdown waveform model for binary black holes (§4.1), and another that focuses only on the inspiral regime of the IMRPhenomD model (§4.2).

4.1 Inspiral-Merger-Ringdown + Dissipation for Binary Black Holes

In this section, we incorporate the tidal dissipation phase contributions (3.56) into IMRPhenomD [147] — a waveform model that describes the inspiral-merger-ringdown of quasi-circular aligned-spins BBHs. By virtue of utilizing the BBH merger and ringdown waveforms in the PE process, we are essentially constraining the dissipation numbers of black holes in this analysis.

Since the tidal dissipation phases (3.56) are only valid in the inspiral portion of the binary waveform, we incorporate them in the IMRPhenomD model at low frequencies terminate their contributions at high frequencies when the binary approaches merger. This is achieved by introducing the taping frequency, f_{22}^{tape} , which is related to the peak frequency at which the (2, 2) radiation mode has maximum amplitude in the merger regime, f_{22}^{peak} , via [148]

$$f_{22}^{\text{tape}} = \alpha f_{22}^{\text{peak}}, \quad (4.1)$$

where the constant $0 < \alpha < 1$ is the parameter. In this work, we choose $\alpha = 0.35$, in line with the analysis conducted by the LVK collaboration in the context of testing theories beyond General Relativity [149, 150]. As discussed in [148], this choice strikes a good balance between utilizing an appreciable portion of the SNR in inspiral portion of the BBH signal while reducing the contributions from the merger, for which our analytic tidal dissipation phases are invalid. We then model the total GW phase in (3.50) as

$$\psi(f) = \begin{cases} \psi^{\text{IMRPhenomD}}(f) + \psi^{\text{TDN}}(f) - \psi^{\text{TDN}}(f_{22}^{\text{ref}}), & f \leq f_{22}^{\text{tape}} \\ \psi^{\text{IMRPhenomD}}(f) + \psi^{\text{TDN}}(f_{22}^{\text{tape}}) - \psi^{\text{TDN}}(f_{22}^{\text{ref}}), & f > f_{22}^{\text{tape}}, \end{cases} \quad (4.2)$$

where the phases are C^0 continuous at $f = f_{22}^{\text{tape}}$. The reference frequency f_{22}^{ref} is the frequency at which the phase of the (22)-mode in IMRPhenomD waveform vanishes, and the value of $\psi^{\text{TDN}}(f_{22}^{\text{ref}})$ acts merely as an overall constant phase and does not impact the PE. In contrast to the flexible theory-independent approach adopted in [151], we do not have to apply a smoothing window near the taping frequency in (4.2) as our waveform model and likelihood evaluations are directly implemented in the frequency domain.

Since our analysis in this section only applies to binary black holes, we will impose the black hole E/B duality (3.61) to reduce the number of free parameters in the PE process. We also assume that the black holes have small spins, $\chi \ll 1$, in order to drop the spin-quadratic, spin-cubic and spin-quartic terms in the EFT decomposition described in §3.1. This simplification has the additional advantage of directly relating the spin-linear $H_{1,2S}$ and spin-independent $H_{1,2\omega}$ dissipation numbers via the superradiance constraint (3.48). As a result, our parameter space spans over 13 dimensions: the independent intrinsic parameters are $\{m_1, m_2, \chi_1, \chi_2, H_{1\omega}, H_{2\omega}\}$, which are described in §3.4, and the extrinsic parameters include $\{D, t_c, \phi_c, \iota, \psi, \alpha, \delta\}$, which are the luminosity distance D , the coalescence time and phase t_c and ϕ_c , the inclination angle ι , the polarization angle ψ , and the right ascension and declination, α and δ respectively. We run our PE studies with `cogwheel` [152], and adopt uniform priors for the detector-frame component masses m_1, m_2 and for the spin components χ_1, χ_2 , with the spin priors spanning over the interval $\mathbf{U}[-0.99, 0.99]$. For the component dissipation parameters $H_{1\omega}, H_{2\omega}$, we use a uniform prior over the range $\mathbf{U}[-5 \times 10^3, 5 \times 10^3]$. All extrinsic parameters are marginalized analytically for fast PE [152].

4.1.1 Constraints for Individual Events

We conduct PE on the BBH events reported in the O1, O2, O3a and O3b IAS catalog with detector frame chirp masses $\mathcal{M} < 40M_\odot$, as these low-mass binaries have non-negligible portions of their signal dominated by the inspiral part of the waveform in the LIGO-Virgo observing band. We focus on the effective dissipation numbers $\mathcal{H}_1, \overline{\mathcal{H}}_1$ and \mathcal{H}_0 as the phase terms in (3.56) suggest that these mass-weighted quantities are better constrained than the component dissipation numbers.

In Fig. 3, we present the marginalized posterior distributions for $\mathcal{H}_1, \overline{\mathcal{H}}_1$ and \mathcal{H}_0 for the seven events for which these coefficients are best constrained: GW200311_115853, GW150914, GW170814, GW190708_232457, GW191216_213338, GW170608, GW200202_154313 (listed in descending order in chirp mass). We observe that these events constrain the dissipation numbers to $|\mathcal{H}_1| \sim |\overline{\mathcal{H}}_1| \sim |\mathcal{H}_0| \lesssim 300$ at the 90% credible interval. The constraints tend to be narrower for lower mass binary systems, which is expected as the signal waveforms are dominated by the inspiral portion of the waveform for low mass binaries in the LIGO-Virgo observation bands. For the best event GW191216_213338, which has a relatively high signal-to-noise ratio of 19.2 and a relatively small median chirp mass $\mathcal{M}_{\text{chirp}} = 8.91_{-0.05}^{+0.07} M_\odot$ and the error bars indicating the 90% credible interval, the constraints are $|\mathcal{H}_1| \sim |\overline{\mathcal{H}}_1| \sim |\mathcal{H}_0| \lesssim 100$. In Figs. 4 and 5, we present the constraints for the remaining BBHs in the IAS event catalog. From these posteriors, it is clear that current detector sensitivities lead to likelihoods that tend to rule out large dissipation values $|\mathcal{H}_1| \sim |\overline{\mathcal{H}}_1| \sim |\mathcal{H}_0| \gtrsim 500$ while the region for smaller values remains prior dominated.

4.1.2 Constraints at the Population Level

We may obtain a stronger constraint on the black hole dissipation numbers by combining the posterior samples for the individual events shown in Fig. 4 and 5, essentially constraining the dissipation numbers at the level of the black hole population. In what follows, we will also constrain the ratio of energy lost due to tidal dissipation from the total energy flux. For simplicity, we will focus on the spin-independent coefficient \mathcal{H}_0 as the results are similar for the other spin-dependent terms.

We conduct the population inference via two approaches: *i*) by computing the joint posterior distribution by multiplying the posterior samples of the individual events, and *ii*) using the hierarchical Bayesian approach [153, 154]. The joint posterior distribution of the BBH events, assuming they are independent, is proportional to the product of the individual likelihoods

$$\mathcal{P}(\mathcal{H}_0|\mathbf{d}) \propto \mathcal{L}(\mathbf{d}|\mathcal{H}_0)\mathcal{P}(\mathcal{H}_0), \quad \mathcal{L}(\mathbf{d}|\mathcal{H}_0) = \prod_{j=1}^N \mathcal{L}(d_j|\mathcal{H}_0), \quad (4.3)$$

where $\mathbf{d} = \{d_j\}$ is the joint data of the individual events and $\mathcal{P}(\mathcal{H}_0)$ is the prior for \mathcal{H}_0 . In the first approach, we multiply the marginalized posterior samples $\mathcal{P}(\mathcal{H}_0|d_j)$ collected for the individual BBH events in §4.1.1, and then reweight the final distribution by dividing it with the prior $\mathcal{P}(\mathcal{H}_0)$ of each event (which are all approximately uniform but can vary slightly from one another because $\mathcal{P}(\mathcal{H}_0)$ depends on mass). The result of this approach is shown in Fig. 6, where the joint constraint is $-6 < \mathcal{H}_0 < 13$ at the 90% credible level. For linear-spin dissipation numbers \mathcal{H}_1 and $\bar{\mathcal{H}}_1$, we obtain the joint constraints $-11 < \mathcal{H}_1 < 6$ and $-11 < \bar{\mathcal{H}}_1 < 9$ at the 90% credible level respectively. Note that by virtue of the central limit theorem, the joint distributions are Gaussian distributed, even though the posteriors of the individual events in Figs. 4 and 5 are generally non-Gaussian.

In the hierarchical combining approach, we infer the joint posterior $\mathcal{P}(\mathcal{H}_0|\mathbf{d})$ by assuming that \mathcal{H}_0 follows an underlying population distribution that is governed by a set of hyperparameters.

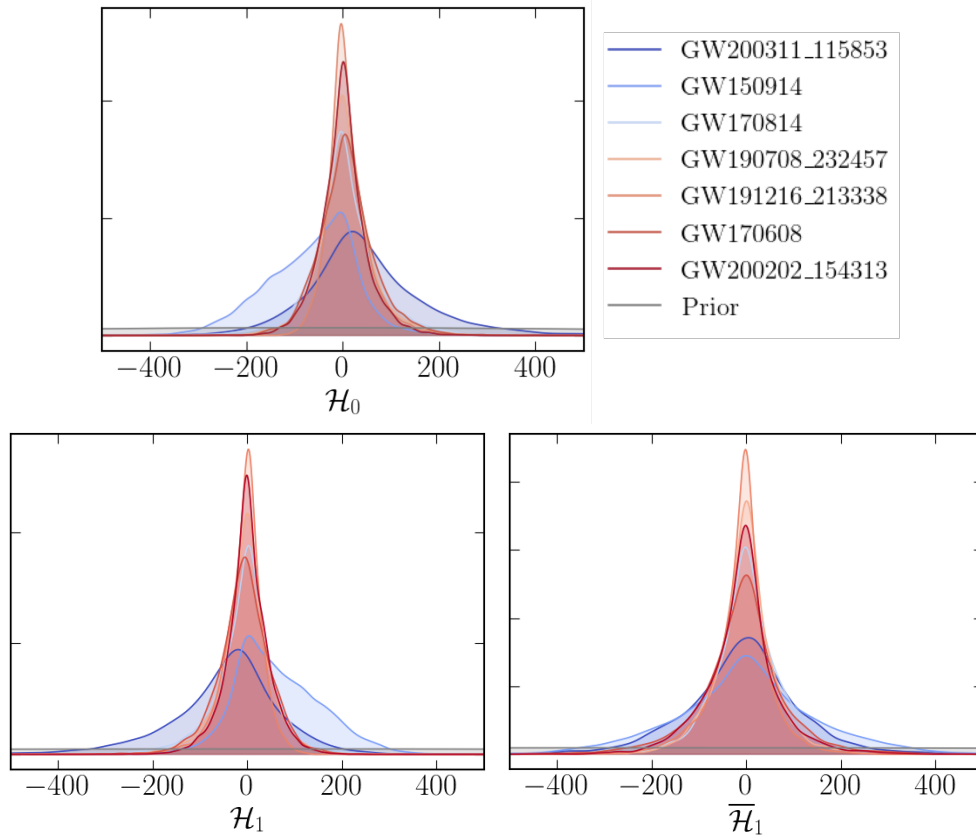


Figure 3: Marginalized posterior distributions for the spin-independent \mathcal{H}_0 , mass-symmetric spin-linear \mathcal{H}_1 , and mass-antisymmetric spin-linear $\bar{\mathcal{H}}_1$ tidal dissipation coefficients for the seven BBH events for which these coefficients are best constrained.

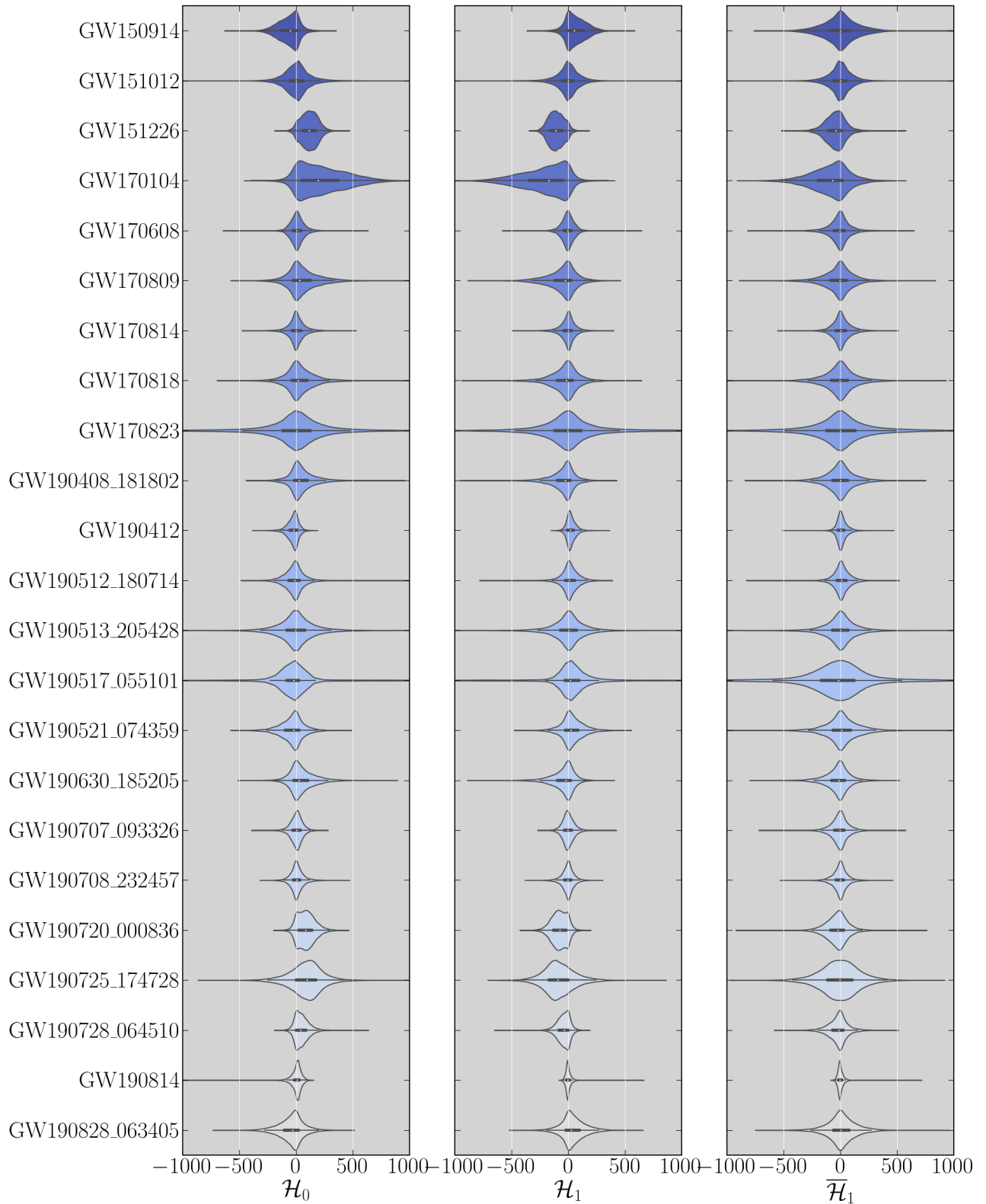


Figure 4: Same as Fig. 3, except here we show the marginalized posteriors for the all the BBHs with detector frame chirp mass $\mathcal{M} < 40M_\odot$ in the IAS O1, O2, O3a and O3b catalog.

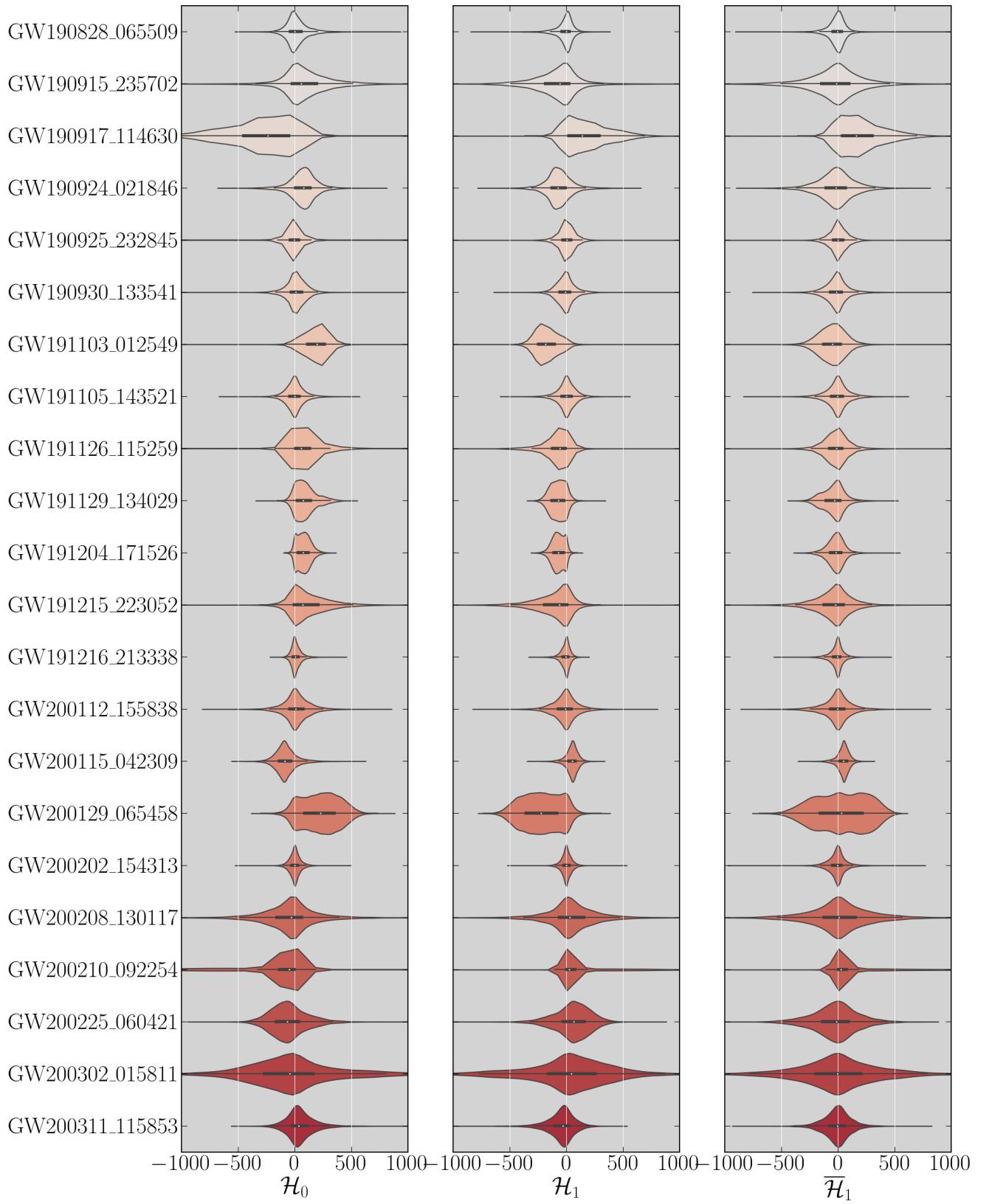


Figure 5: Continuation of Fig. 4.

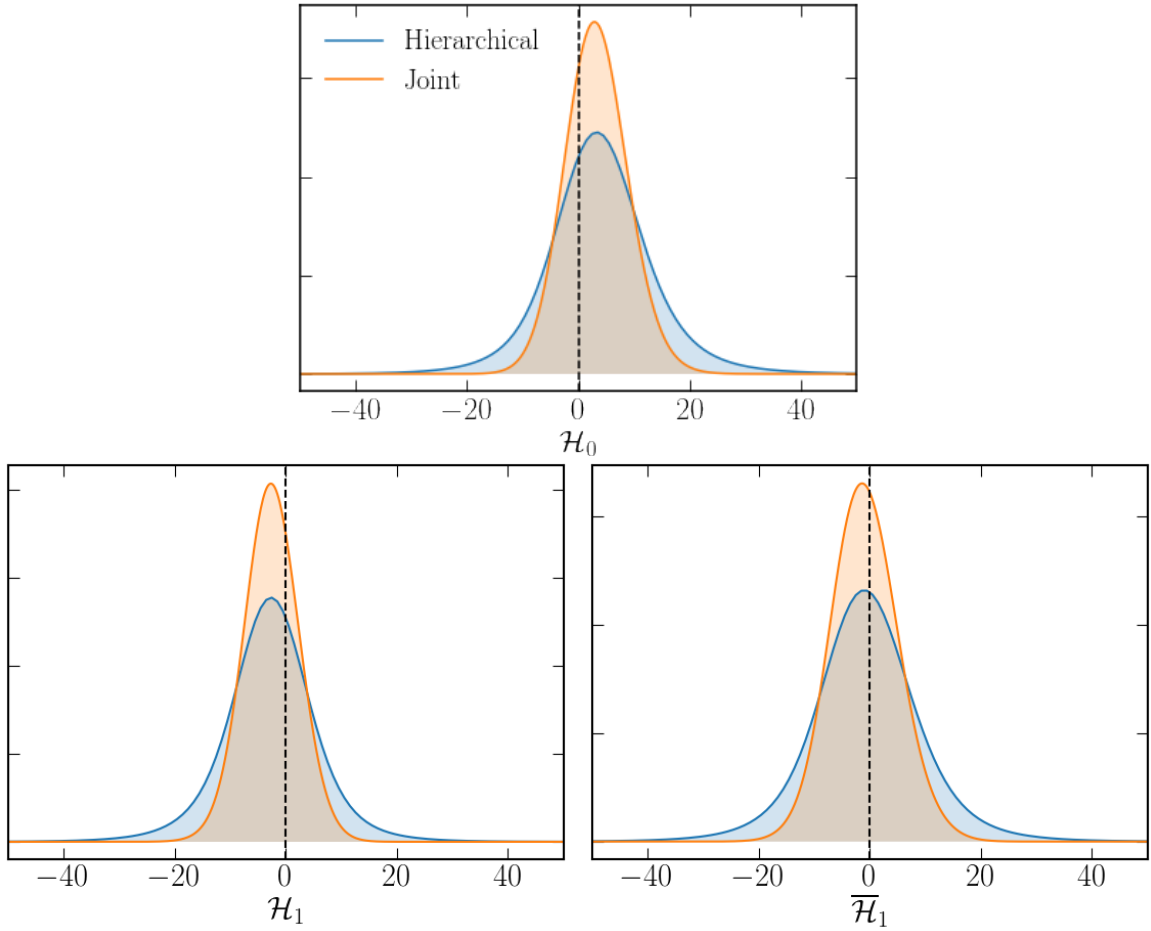


Figure 6: Constraints on \mathcal{H}_0 , \mathcal{H}_1 and $\bar{\mathcal{H}}_1$ of the BBH population. We present results for the joint posterior distribution and the posterior computed using the hierarchical Bayesian approach. The black dashed lines represent the theoretical GR prediction for black holes.

In this work, we assume that \mathcal{H}_0 is Gaussian distributed with mean μ and standard deviation σ at the population level:

$$\mathcal{P}(\mathcal{H}_0|\mu, \sigma) = \mathcal{N}(\mathcal{H}_0|\mu, \sigma^2) , \quad (4.4)$$

The joint posterior $\mathcal{P}(\mathcal{H}_0|\mathbf{d})$ would be obtained by marginalizing over the posterior distribution on these hyperparameters

$$\mathcal{P}(\mathcal{H}_0|\mathbf{d}) = \int \mathcal{P}(\mathcal{H}_0|\mu, \sigma) \mathcal{P}(\mu, \sigma|\mathbf{d}) d\mu d\sigma . \quad (4.5)$$

From Bayes rule, $\mathcal{P}(\mu, \sigma|\mathbf{d})$ can be computed as follow:

$$\mathcal{P}(\mu, \sigma|\mathbf{d}) \propto \mathcal{L}(\mathbf{d}|\mu, \sigma) \mathcal{P}(\mu, \sigma) , \quad \mathcal{P}(\mathbf{d}|\mu, \sigma) = \prod_{j=1}^N \mathcal{L}(d_j|\mu, \sigma) . \quad (4.6)$$

where the likelihood for the individual events for a given set of $\{\mu, \sigma\}$ is obtained by marginalizing over the dissipation number posterior distribution of the individual events, \mathcal{H}_0^j :

$$\mathcal{L}(d_j|\mu, \sigma) = \int \mathcal{L}(d_j|\mathcal{H}_0^j) \mathcal{P}(\mathcal{H}_0^j|\mu, \sigma) d\mathcal{H}_0^j . \quad (4.7)$$

Strictly speaking, the likelihood of the individual event in the integrand above should be $\mathcal{L}(d_j|\mathcal{H}_0^j, \mu, \sigma)$. However, since $\mathcal{L}(d_j|\mathcal{H}_0^j, \mu, \sigma)$ cannot be directly computed, the conditional dependence on $\{\mu, \sigma\}$ is dropped – this is the essence of hierarchical Bayesian inference. We compute $\mathcal{L}(d_j|\mathcal{H}_0^j)$ by dividing the marginalized posteriors in Figs. 4 and 5 by the prior of the individual events $\mathcal{P}(\mathcal{H}_0^j)$ in the PE. Because we assume that the observed distribution on \mathcal{H}_0^j arises from an underlying population, we take $\mathcal{P}(\mathcal{H}_0^j|\mu, \sigma) = \mathcal{P}(\mathcal{H}_0|\mu, \sigma)$ in (4.7). Finally, to compute (4.6) we choose the hyperprior $\mathcal{P}(\mu, \sigma) = \mathcal{P}(\mu)\mathcal{P}(\sigma)$ to be independent and uniformly distributed, with $\mu \sim \mathbf{U}[-40, 40]$ and $\sigma \sim \mathbf{U}[0, 30]$. The results of the hierarchical approach is also shown in the left panel of Fig. 6, where we find that the joint constraint is very similar to that from direct multiplications, with $-13 < \mathcal{H}_0 < 20$, $-18 < \mathcal{H}_1 < 11$ and $-18 < \tilde{\mathcal{H}}_1 < 16$ at the 90% credible level.

Finally, we use the same two approaches outlined above to constrain the ratio of the energy loss due to tidal dissipation, ΔE_{H} , to the energy loss at infinity, ΔE_{∞} (see (A.23) in Appendix A for details of the computation). This ratio provides an alternative and more physically interpretable way of understanding the importance of tidal dissipation in the binary dynamics. The results are shown in Fig. 1, where the constraint of $\Delta E_{\text{H}}/\Delta E_{\infty}$ at the population level is $-0.0026 < \Delta E_{\text{H}}/\Delta E_{\infty} < 0.0025$ at 90% credible level using the hierarchical approach. This finding is consistent with the GR prediction that BBHs would lose approximately a fraction of $\sim 10^{-5} - 10^{-4}$ of its energy to tidal dissipation compared to the radiation at infinity.

4.2 Inspiral-only + Dissipation for Exotic Binaries

Unlike in §4.1, where we used the full inspiral-merger-ringdown waveforms of IMRPhenomD as a baseline model, in this section we restrict ourselves only to the inspiral regime of IMRPhenomD. This inspiral-only waveform, which is similar to the analytic TaylorF2 waveform model [144, 155] up to non-perturbative resummations of non-linear effects such as through Padé resummation [156, 157] and parameterized higher PN terms [147, 158], applies to the quasi-circular inspiral of all types of binary systems, including binary black holes and exotic binary systems. As a result, we *do not* assume that the signals in the GW catalog are sourced by BBHs in this section. This inspiral-only analysis allows us to present our results as general constraints that apply to all types of exotic compact binary coalescences.

In order to focus on the inspiral regime, we project out the merger-ringdown portions in both the data, d , and the IMRPhenomD model, h . More precisely, we achieve this projection by truncating both d and h in the frequency domain via the new likelihood

$$\log \mathcal{L}_{\text{new}} = \langle d|\mathbb{P}|h \rangle - \frac{1}{2} \langle h|\mathbb{P}|h \rangle, \quad (4.8)$$

where the projection operator \mathbb{P} is a top hat window function in Fourier space

$$\langle a|\mathbb{P}|b \rangle \equiv 4 \operatorname{Re} \int_{f_{\min}}^{f_{22}^{\text{tape}}} \frac{\tilde{a}^*(f)\tilde{b}(f)}{S_n(f)}, \quad (4.9)$$

with $f_{\min} = 20\text{Hz}$ being the minimum frequency and f_{22}^{tape} is the tapering frequency in (4.1), which determines the frequency range at which the binary inspiral is separated from the merger and ringdown.

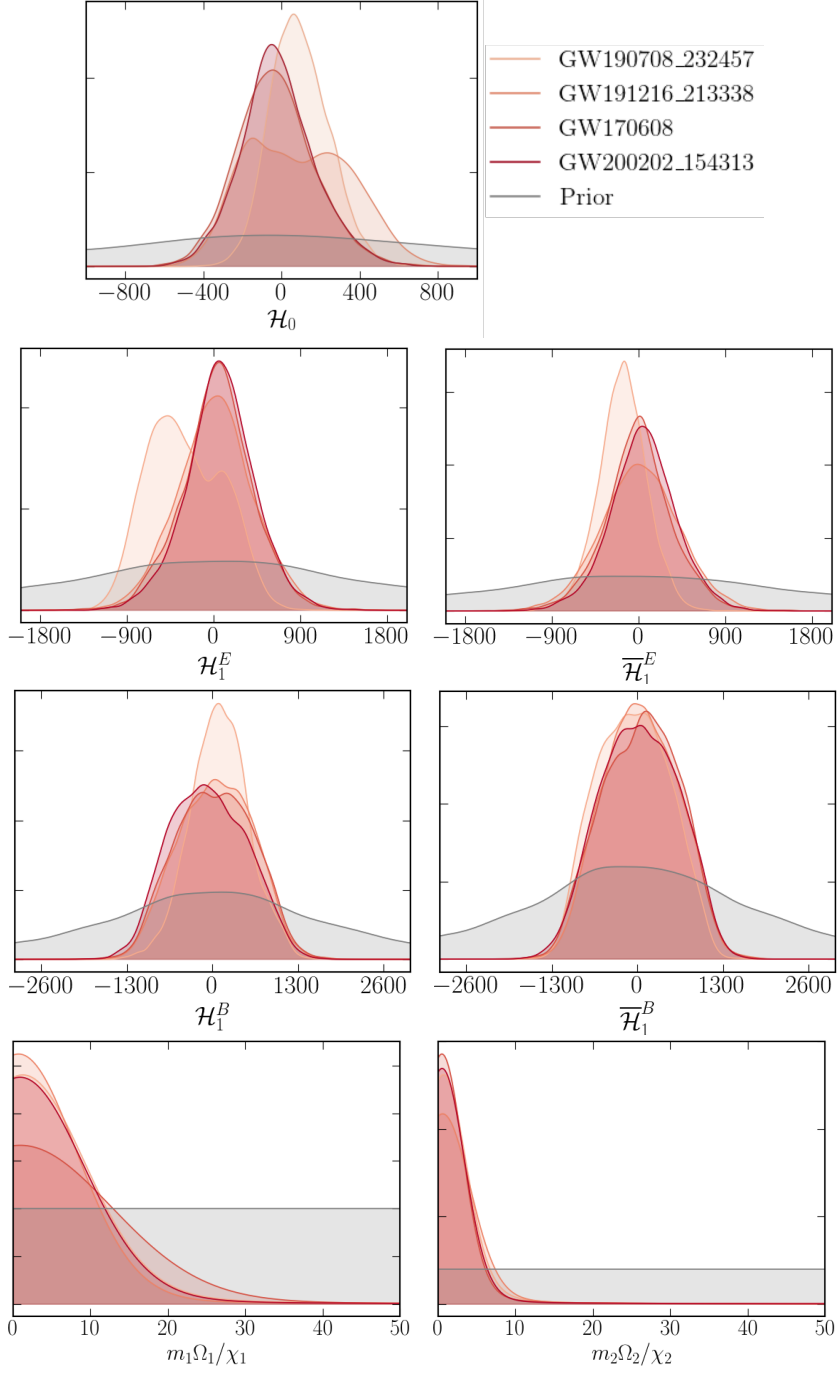


Figure 7: Similar to Fig. 3, except here we incorporate the tidal dissipation coefficients in a baseline model which consists only of the inspiral regime of IMRPhenomD (we only show the same four events with $\mathcal{M} < 25M_\odot$). Since the inspiral-only waveform applies not only to binary black holes but also to all types of binary coalescences, we present these results as general constraints for exotic compact objects. Since all astrophysical objects other than black holes do not respect E/B duality, we treat the electric (second row) and magnetic (third row) linear-spin dissipation numbers separately. In the final row, we include the posteriors for dimensionless angular velocity of the two compact objects.

Since we do not assume that the signals arise from black holes, we do not impose the E/B duality in the following PE analysis. We still assume the objects have small spins, $\chi \ll 1$, in order to ignore the spin-quadratic, spin-cubic and spin-quartic dissipation terms. Having said that, the superradiance relation (3.47) for a general object in the $\chi \ll 1$ limit would not directly relate the spin-linear and spin-independent terms due to the presence of Ω as another free parameter. As a result, our parameter space is now widened to 17 dimensions, where the extrinsic parameters are the same as before and the independent intrinsic parameters are $\{m_1, m_2, \chi_1, \chi_2, H_{1S}^B, H_{2S}^B, H_{1\omega}, H_{2\omega}, \Omega_1, \Omega_2\}$. We use flat prior for the dimensionless angular momentum $m_i \Omega_i / \chi_i \sim \mathbf{U}[0, 10^2], i = 1, 2$.

In Fig. 7, we show the marginalized posterior distributions of the spin-independent dissipation number \mathcal{H}_0 , the electric and magnetic, mass-symmetric and antisymmetric linear-spin dissipation numbers, $\mathcal{H}_1^{E,B}, \overline{\mathcal{H}}_1^{E,B}$. We present the results for the same four lightest events shown in Fig. 3 and omit the heavier events with $\mathcal{M} > 25M_\odot$, as the waveforms of these events in the LIGO-Virgo observing bands are dominated by the merger regime where our inspiral-only waveform is invalid. The constraints are now manifestly wider than those in Fig. 3; for instance, we find $|\mathcal{H}_0| \lesssim 400$ at 90% credible interval here compared to the 90% credible bound of $|\mathcal{H}_0| \lesssim 100$ in the inspiral-merger-ringdown analysis in §4.1.1. The broader posteriors here arise due to the reduced SNR in the likelihood evaluation for the inspiral-only waveform. In particular, since the effective dissipation numbers depend on mass, the lack of merger implies the masses are less precisely measured, resulting in broader posterior distributions in the dissipation numbers.

It is also important to emphasize that, without imposing the kinematic superradiance constraint in this section, \mathcal{H}_0 is more precisely measured than the linear-spin dissipation numbers even though \mathcal{H}_0 formally appears at 4PN in the waveform phase while the linear-spin terms first appear at a lower 2.5PN order. This is because spins are not very precisely measured by current detectors, and most of the inferred spins are consistent with zero. This key observation motivates \mathcal{H}_0 as the most well motivated target parameter in studies of tidal dissipation in binary systems. Indeed, \mathcal{H}_0 directly plays an analogous role to the effective tidal Love parameter Λ , which is the leading tidal deformability parameter in GW analysis.

In addition, notice that the magnetic dissipation numbers are less well-constrained than the electric counterparts, as is expected because the former first appears at a higher order of 3.5PN while the latter first appear at 2.5PN order (see Table 2 for summary). Note that we do not assume here that these exotic binary systems arise from the same underlying population, i.e. unlike §4.1.2 we do not conduct a population study in this section.

5 Conclusions and Outlook

In this paper, we present the first rigorous derivation of tidal dissipation of a general rotating body and their associated impacts on GW observables in merging binary systems. Our approach utilizes the worldline EFT framework, whereby the spin-dependent and spin-independent tidal dissipation coefficients are inferred as operators that break time-reversal symmetry in the retarded tidal response function. A summary of the linear-spin, cubic-spin and spin-independent effective dissipation numbers that are best measured in binary systems are shown in (3.57). We also derived the tidal heating imprints on the GW phases and amplitudes for quasi-circular orbits; these results are presented in (3.56) and (3.60). These results *a priori* make no assumption

about the nature of the binary components and can therefore be used to test all types of binary constituents, including black holes, neutron stars and other types of exotic compact objects. If one assumes that the binary source is a BBH, one may reduce the dimensionality of the parameter space by imposing the black hole electric-magnetic duality (3.61). In this case the tidal heating phase imprints simplify slightly, and we list them in (3.62) for convenience.

A summary of our PE constraints are presented in Table 2, with further details of the methods and results elaborated in Section 4. For BBHs, we evaluated the posterior distributions of the dissipation numbers in Figs. 3, 4 and 5 for the BBHs in the O1-O3 catalog. We further combined these posteriors and obtain a joint posterior on \mathcal{H}_0 , obtaining the BBH population constraint of $-13 < \mathcal{H}_0 < 20$ at the 90% credible level shown in Fig. 6. While this result is still two orders of magnitude larger than the theoretical value of $\mathcal{H}_0 = 2/45 \approx 4.4 \times 10^{-2}$ for equal mass BBH, future GW observations with improved detector sensitivity and rapidly increasing number of detections will significantly improve upon current constraints. On the other hand, if we do not assume that the binaries are BBHs, the constraints on the electric and magnetic dissipation numbers are relaxed by an approximately an order of magnitude; see Fig. 7 for the posteriors for a select few events. These results can be interpreted as constraints imposed on exotic types of binary systems as the BH electric-magnetic duality are not imposed in the PE computation.

Our work represents the first holistic treatment of tidal heating effects in GW binary sources. In a way, the derivation of the effective dissipation numbers in our work completes the long-standing goal of finding physically-motivated parameterizations of all leading order finite-size effects of compact binary coalescence. Along with the spin-induced multipole moments and the tidal deformability parameters, we are now well-equipped to build GW models which incorporate all finite-size effects of astrophysical bodies as free parameters in the waveforms. Such waveform models would offer a robust and theoretically-consistent framework for probing new types of compact binary systems: both at the search level, such as a recent work dedicated to searching for compact objects with large Love numbers [12], and for accurate parameter estimations to test for new physics [150]. As the LVK detector sensitivity improves over time and we observe more high signal-to-noise ratio events, it would also be interesting to apply our results in this work to further measure or constrain the dissipation numbers of BBHs. We intend to pursue these interesting research directions in future work.

Acknowledgments

We thank Anna Biggs, Jingping Li, Ajit Kumar Mehta, Julio Parra-Martinez, Irvin Martínez-Rodríguez, Javier Roulet, Muddu Saketh and Matias Zaldarriaga for stimulating discussions. HSC gratefully acknowledges support from the Ambrose Monell Foundation and the Sivian Fund at the Institute for Advanced Study.

This research has made use of data, software and/or web tools obtained from the Gravitational Wave Open Science Center (<https://www.gw-openscience.org/>), a service of LIGO Laboratory, the LIGO Scientific Collaboration and the Virgo Collaboration. LIGO Laboratory and Advanced LIGO are funded by the United States National Science Foundation (NSF) as well as the Science and Technology Facilities Council (STFC) of the United Kingdom, the Max-Planck-Society (MPS), and the State of Niedersachsen/Germany for support of the construction of Advanced

LIGO and construction and operation of the GEO600 detector. Additional support for Advanced LIGO was provided by the Australian Research Council. Virgo is funded, through the European Gravitational Observatory (EGO), by the French Centre National de Recherche Scientifique (CNRS), the Italian Istituto Nazionale di Fisica Nucleare (INFN) and the Dutch Nikhef, with contributions by institutions from Belgium, Germany, Greece, Hungary, Ireland, Japan, Monaco, Poland, Portugal, Spain.

A Derivation of Waveform Observables

In this appendix, we present the derivation for the TaylorF2 waveform phase and amplitude which includes arbitrary values of dissipation constants — up to 3.5PN order for spin-dependent dissipation terms and up to 4PN order for the spin-independent terms. The basic inputs in the derivation are the binding energy \mathcal{E} , the energy flux at infinity \mathcal{F}_∞ , and the tidal heating energy fluxes for the binary components \dot{m}_1 and \dot{m}_2 .

Since our focus is on tidal heating of general rotating bodies, for simplicity we restrict ourselves to the expressions derived for black holes in \mathcal{E} and \mathcal{F}_∞ . For example, for the spin-spin interaction terms we set the spin-induced moments [26] to the black hole value [159–161]. On the other hand, for \dot{m}_1 and \dot{m}_2 we present the derivations for general rotating bodies. This will allow us to present the tidal dissipation imprints on the phase and amplitude for both general binary systems and for BBHs.

We restrict ourselves to aligned-spin orbits by using the following spin variables

$$\begin{aligned} S_\ell &= \frac{\boldsymbol{\ell} \cdot \mathbf{S}}{GM^2} = \frac{1}{4} [(1 + \delta)^2 \chi_1 + (1 - \delta)^2 \chi_2] , \\ \Sigma_\ell &= \frac{\boldsymbol{\ell} \cdot \boldsymbol{\Sigma}}{GM^2} = -\frac{1}{2} [(1 + \delta)\chi_1 - (1 - \delta)\chi_2] , \end{aligned} \tag{A.1}$$

where $\boldsymbol{\ell}$ is the orbital angular momentum normal vector and the spin vectors are

$$\mathbf{S} = \mathbf{S}_1 + \mathbf{S}_2 , \quad \boldsymbol{\Sigma} = M \left(\frac{\mathbf{S}_2}{m_2} - \frac{\mathbf{S}_1}{m_1} \right) . \tag{A.2}$$

Furthermore, we restrict ourselves to the (2, 2) radiation mode. This implies that the orbital velocity, which is the PN perturbation parameter, is $v = (\pi M f)^{1/3}$. Finally, we assume the orbits are quasicircular.

Binding Energy

We express the binding energy as

$$\mathcal{E}(v) = -\frac{M\eta v^2}{2} [\mathcal{E}_{\text{NS}}(v) + \mathcal{E}_{\text{SO}}(v)v^3 + \mathcal{E}_{\text{SS}}(v)v^4 + \mathcal{E}_{\text{SSS}}(v)v^7] , \tag{A.3}$$

where the non-spinning point-particle contribution E_{NS} is shown up to 4PN [146]:

$$\begin{aligned}
\mathcal{E}_{\text{NS}}(v) = & 1 - \left(\frac{3}{4} + \frac{1}{12}\eta \right) v^2 - \left(\frac{27}{8} - \frac{19}{8}\eta + \frac{1}{24}\eta^2 \right) v^4 \\
& - \left\{ \frac{675}{64} - \left(\frac{34445}{576} - \frac{205}{96}\pi^2 \right) \eta + \frac{155}{96}\eta^2 + \frac{35}{5184}\eta^3 \right\} v^6 \\
& + \left\{ -\frac{3969}{128} + \left[-\frac{123671}{5760} + \frac{9037}{1536}\pi^2 + \frac{896}{15}\gamma_{\text{E}} + \frac{896}{15}\ln(4v) \right] \eta \right. \\
& \left. + \left[-\frac{498449}{3456} + \frac{3157}{576}\pi^2 \right] \eta^2 + \frac{301}{1728}\eta^3 + \frac{77}{31104}\eta^4 \right\} v^8.
\end{aligned} \tag{A.4}$$

The logarithmic term above arises from the tail effect to the radiation-reaction potential. The binding energy from spin-orbital coupling is

$$\begin{aligned}
\mathcal{E}_{\text{SO}}(v) = & \left(\frac{14}{3}S_{\ell} + 2\delta\Sigma_{\ell} \right) + \left[\left(11 - \frac{61}{9}\eta \right) S_{\ell} + \left(3 - \frac{10}{3}\eta \right) \delta\Sigma_{\ell} \right] v^2 \\
& + \left[\left(\frac{135}{4} - \frac{367}{4}\eta + \frac{29}{12}\eta^2 \right) S_{\ell} + \left(\frac{27}{4} - 39\eta + \frac{5}{4}\eta^2 \right) \delta\Sigma_{\ell} \right] v^4.
\end{aligned} \tag{A.5}$$

Taking the spin-induced quadrupole and octupole to be the black hole values [159–161], the quadratic-in-spin contribution to the binding energy is

$$\begin{aligned}
\mathcal{E}_{\text{SS}}(v) = & -4S_{\ell}^2 - 4\delta S_{\ell}\Sigma_{\ell} + (-1 + 4\eta)\Sigma_{\ell}^2 \\
& + \left[S_{\ell}^2 \left(-\frac{25}{9} + \frac{10\eta}{3} \right) + S_{\ell} \left(\frac{10\delta}{3} + \frac{10\delta\eta}{3} \right) \Sigma_{\ell} + \left(\frac{5}{2} - \frac{15\eta}{2} - \frac{10\eta^2}{3} \right) \Sigma_{\ell}^2 \right] v^2,
\end{aligned} \tag{A.6}$$

whereas the cubic-in-spin terms are

$$\mathcal{E}_{\text{SSS}}(v) = -8S_{\ell}^3 - 16\delta S_{\ell}^2\Sigma_{\ell} + (-10 + 40\eta)S_{\ell}\Sigma_{\ell}^2 + (-2\delta + 8\delta\eta)\Sigma_{\ell}^3. \tag{A.7}$$

Energy Flux at Infinity

The energy flux radiated to infinity is organized as

$$\mathcal{F}_{\infty}(v) = \frac{32}{5}\eta^2 v^{10} [\mathcal{F}_{\text{NS}}(v) + \mathcal{F}_{\text{SO}}(v)v^3 + \mathcal{F}_{\text{SS}}(v)v^4 + \mathcal{F}_{\text{SSS}}(v)v^7], \tag{A.8}$$

where $\mathcal{F}_{\text{NS}}(v)$ has recently been derived up to 4PN [19, 20]

$$\begin{aligned}
\mathcal{F}_{\text{NS}}(v) = & 1 + \left(-\frac{1247}{336} - \frac{35}{12}\eta\right)v^2 + 4\pi v^3 + \left(-\frac{44711}{9072} + \frac{9271}{504}\eta + \frac{65}{18}\eta^2\right)v^4 \\
& + \left(-\frac{8191}{672} - \frac{583}{24}\eta\right)\pi v^5 + \left[\frac{6643739519}{69854400} + \frac{16}{3}\pi^2 - \frac{1712}{105}\gamma_E - \frac{1712}{105}\ln(4v)\right. \\
& + \left(-\frac{134543}{7776} + \frac{41}{48}\pi^2\right)\eta - \frac{94403}{3024}\eta^2 - \frac{775}{324}\eta^3\left. \right]v^6 + \left(-\frac{16285}{504} + \frac{214745}{1728}\eta\right. \\
& + \left.\frac{193385}{3024}\eta^2\right)\pi v^7 + \left[-\frac{323105549467}{3178375200} + \frac{232597}{4410}\gamma_E - \frac{1369}{126}\pi^2 + \frac{39931}{294}\ln 2\right. \\
& - \frac{47385}{1568}\ln 3 + \frac{232597}{4410}\ln v + \left(-\frac{1452202403629}{1466942400} + \frac{41478}{245}\gamma_E - \frac{267127}{4608}\pi^2\right. \\
& + \left.\frac{479062}{2205}\ln 2 + \frac{47385}{392}\ln 3 + \frac{41478}{245}\ln v\right)\eta + \left(\frac{1607125}{6804} - \frac{3157}{384}\pi^2\right)\eta^2 \\
& + \left.\frac{6875}{504}\eta^3 + \frac{5}{6}\eta^4\right]v^8.
\end{aligned} \tag{A.9}$$

The logarithmic term which appears at 3PN arises from the tail effect of the renormalization group (RG) running of the quadrupole moment. At 4PN, not only are there the RG contributions but also the tail-of-memory effects [19, 20]. The spin-orbital coupling contribution to the flux at infinity is

$$\begin{aligned}
\mathcal{F}_{\text{SO}}(v) = & -4S_\ell - \frac{5\delta\Sigma_\ell}{4} + v^2 \left[\left(-\frac{9}{2} + \frac{272\eta}{9}\right)S_\ell + \left(-\frac{13\delta}{16} + \frac{43\delta\eta}{4}\right)\Sigma_\ell \right] \\
& - 16\pi v^3 S_\ell - \frac{31\delta\pi\Sigma_\ell v^3}{6} \\
& + v^4 \left[\left(\frac{476645}{6804} + \frac{6172\eta}{189} - \frac{2810\eta^2}{27}\right)S_\ell + \left(\frac{9535\delta}{336} + \frac{1849\delta\eta}{126} - \frac{1501\delta\eta^2}{36}\right)\Sigma_\ell \right],
\end{aligned} \tag{A.10}$$

Similar to the binding energy, we take the black hole spin-induced multipole moment values [159–161] for the spin-spin contributions to the flux. For quadratic spins, this is

$$\begin{aligned}
\mathcal{F}_{\text{SS}}(v) = & 8S_\ell^2 + 8\delta S_\ell \Sigma_\ell + \left(\frac{33}{16} - 8\eta\right)\Sigma_\ell^2 \\
& + \left(\left(-\frac{3839}{252} - 43\eta\right)S_\ell^2 + \left(-\frac{1375\delta}{56} - 43\delta\eta\right)S_\ell \Sigma_\ell + \left(-\frac{227}{28} + \frac{3481\eta}{168} + 43\eta^2\right)\Sigma_\ell^2\right)v^2 \\
& + \left(32\pi S_\ell^2 + 32\delta\pi S_\ell \Sigma_\ell + \left(\frac{65\pi}{8} - 32\eta\pi\right)\Sigma_\ell^2\right)v^3,
\end{aligned} \tag{A.11}$$

while the spin-cubic interaction is given by

$$\mathcal{F}_{\text{SSS}}(v) = -\frac{16}{3}S_\ell^3 + \frac{2}{3}\delta S_\ell^2 \Sigma_\ell + \left(\frac{9}{2} - \frac{56\eta}{3}\right)S_\ell \Sigma_\ell^2 + \left(\frac{35\delta}{24} - 6\delta\eta\right)\Sigma_\ell^3. \tag{A.12}$$

Energy Flux from Tidal Heating

From the effective action (3.7), we derive the tidal heating energy flux of a single body, which is equivalent to the equation of motion of the effective action. For a general tidal environment, this

energy flux is

$$\begin{aligned} \dot{m} = -m(Gm)^4 & \left[H_S^E \chi \left(\dot{E}^{ij} E_i^k \hat{S}_{jk} \right) - (Gm) H_\omega^E \dot{E}^{ij} \dot{E}_{ij} \right. \\ & \left. + H_S^B \chi \left(\dot{B}^{ij} B_i^k \hat{S}_{jk} \right) - (Gm) H_\omega^B \dot{B}^{ij} \dot{B}_{ij} \right]. \end{aligned} \quad (\text{A.13})$$

and angular momentum flux

$$\begin{aligned} \dot{J} = -m(Gm)^4 & \left[-2H_S^E \chi \left(E^{ij} E_{ij} \right) + 3H_S^E \chi \left(E_i^k E_{jk} \hat{s}^i \hat{s}^j \right) + (GM) H_\omega^E \left(\dot{E}^{ij} E_i^k \hat{S}_{jk} \right) \right. \\ & \left. - 2H_S^B \chi \left(B^{ij} B_{ij} \right) + 3H_S^B \chi \left(B_i^k B_{jk} \hat{s}^i \hat{s}^j \right) + (GM) H_\omega^B \left(\dot{B}^{ij} B_i^k \hat{S}_{jk} \right) \right], \end{aligned} \quad (\text{A.14})$$

where the J is the dimensionful spin $J \equiv Gm^2 \chi$. For a quasi-circular aligned-spin orbit, the tidal moments E_{ij} and B_{ij} have been computed up to $\mathcal{O}(v^3)$ and $\mathcal{O}(v)$ beyond leading order [162–164], which are sufficiently high PN order for our purposes; see (30)–(34) in [164]. Substituting these tidal moments into (A.13), we obtain the tidal heating flux for m_1 :

$$\begin{aligned} \dot{m}_1(v) = & \left(\frac{9H_{1S}^E m_1^3 \eta^2 \chi_1}{M^3} \right) v^{15} + \left(-\frac{9H_{1S}^E m_1^3 (-2M - m_1 + 3M\eta) \eta^2 \chi_1}{M^4} \right. \\ & \left. + \frac{9H_{1S}^B m_1^3 \eta^2 \chi_1}{M^3} \right) v^{17} + \left(\frac{18H_{1\omega} m_1^4 \eta^2}{M^4} \right) v^{18}. \end{aligned} \quad (\text{A.15})$$

The expression for \dot{m}_2 is obtained by interchanging the $1 \leftrightarrow 2$ indices. The total tidal heating flux absorbed by both binary components, $\dot{M} = \dot{m}_1 + \dot{m}_2$, is therefore

$$\begin{aligned} \dot{M}(v) = & \left(9\overline{\mathcal{H}}_1^E \eta^2 \chi_a + 9\mathcal{H}_1^E \eta^2 \chi_s \right) v^{15} + \left[\left(9\mathcal{H}_1^B \eta^2 + \frac{45\mathcal{H}_1^E \eta^2}{2} + \frac{9}{2} \overline{\mathcal{H}}_1^E \delta \eta^2 - 27\mathcal{H}_1^E \eta^3 \right) \chi_s \right. \\ & \left. + \left(9\overline{\mathcal{H}}_1^B \eta^2 + \frac{45\overline{\mathcal{H}}_1^E \eta^2}{2} + \frac{9}{2} \mathcal{H}_1^E \delta \eta^2 - 27\overline{\mathcal{H}}_1^E \eta^3 \right) \chi_a \right] v^{17} + 18\mathcal{H}_0 \eta^2 v^{18}, \end{aligned} \quad (\text{A.16})$$

where $\mathcal{H}_1^{E/B}$, $\overline{\mathcal{H}}_1^{E/B}$ and $\mathcal{H}_0^{E/B}$ are the effective dissipation numbers defined in (3.57). When studying binary black holes, (A.15) and (A.16) can be simplified via the electric-magnetic duality, $\mathcal{H}_1^E = \mathcal{H}_1^B$, $\overline{\mathcal{H}}_1^E = \overline{\mathcal{H}}_1^B$ and $\mathcal{H}_0^E = \mathcal{H}_0^B$ described in Section 3, with their theoretical values found in (3.45).

GW Phase

Using the results shown above, we may derive the analytic expressions for waveform observables. In particular, the derivation for both the phase and amplitude utilize the energy balance equation:

$$-\mathcal{F}_\infty - \dot{M} = \dot{\mathcal{E}}. \quad (\text{A.17})$$

To compute the phase, one has to solve for the GW orbital phase $\phi(v)$ and time $t(v)$ as observed at asymptotic infinity [144]. Since $\tau \rightarrow t$ at asymptotic infinity, in what follows we reuse overdots for derivative in t for notational simplicity. For quasi-circular orbits, the orbital phase can be

solved via Kepler's third law, which gives $\dot{\phi} = v^3/M$ for the $m_\phi = 2$ radiation mode. Integrating over the equations iteratively, we have

$$t(v) = t_0 + \int dv \frac{1}{\dot{v}}, \quad \phi(v) = \phi_0 + \int dv \frac{v^3}{M \dot{v}}. \quad (\text{A.18})$$

The expression for \dot{v} can be obtained by applying chain rule to $\dot{\mathcal{E}}$ in (A.17) – see also (3.53) – and reorganizing it as follows:

$$\dot{v} = - \left(\frac{\partial \mathcal{E}}{\partial v} \right)^{-1} \left[\mathcal{F}_\infty + \left(1 - \frac{\partial \mathcal{E}}{\partial m_1} \right) \dot{m}_1 + \left(1 - \frac{\partial \mathcal{E}}{\partial m_2} \right) \dot{m}_2 \right], \quad (\text{A.19})$$

whose explicit result for quasicircular orbits can be computed by substituting (A.3), (A.8) and (A.15). As described in the main text, in addition to the fluxes \dot{m}_1 and \dot{m}_2 which are directly absorbed by the binary components, there are also the so-called ‘‘secular change in mass’’ terms arising from applying chain rule to the energy balance equation. Since the leading binding energy scales as $\mathcal{E} \propto v^2$, cf. (A.3), these secular corrections are 1PN suppressed compared $\dot{m}_{1,2}$.

Solving (A.18) iteratively after performing a Taylor expansion on (A.19), we arrive at the TaylorF2 waveform phase for the (2, 2) radiation mode, where $\psi(v) = 2\pi f t(v) - 2\phi(v)$ is the phase in the stationary phase approximation and $v = (\pi M f)^{1/3}$ cf. (3.50). We separate the phase into the point particle (black hole) and the tidal dissipation number contributions:

$$\psi(v) = 2\pi f t_0 - \phi_0 - \frac{\pi}{4} + \frac{3}{128\eta v^5} \left[\psi^{\text{PP}}(v) + \psi^{\text{TDN}}(v) \right], \quad (\text{A.20})$$

where the tidal dissipation terms are shown in (3.55) and (3.56), while the point particle phase contribution is

$$\begin{aligned} \psi^{\text{PP}}(v) = & 1 + v^2 \psi_{1\text{PN}}^{\text{PP}} + v^3 \psi_{1.5\text{PN}}^{\text{PP}} + v^4 \psi_{2\text{PN}}^{\text{PP}} + v^5 (1 + 3 \ln v) \psi_{2.5\text{PN}}^{\text{PP}} + v^6 \psi_{3\text{PN}}^{\text{PP}} \\ & + v^6 \ln v \psi_{3\text{PN}}^{\text{PP,ln}} + v^7 \psi_{3.5\text{PN}}^{\text{PP}} + v^8 (1 - 3 \ln v) \psi_{4\text{PN}}^{\text{PP}} + v^8 (\ln v)^2 \psi_{4\text{PN}}^{\text{PP,ln}^2}, \end{aligned} \quad (\text{A.21})$$

with the PN coefficients [18, 146]

$$\begin{aligned} \psi_{1\text{PN}}^{\text{PP}} &= \frac{3715}{756} + \frac{55\eta}{9}, \\ \psi_{1.5\text{PN}}^{\text{PP}} &= -16\pi + \left(\frac{113}{3} - \frac{76\eta}{3} \right) \chi_s + \frac{113\delta\chi_a}{3}, \\ \psi_{2\text{PN}}^{\text{PP}} &= \frac{15293365}{508032} + \frac{27145\eta}{504} + \frac{3085\eta^2}{72} - \left(\frac{405}{8} - 200\eta \right) \chi_a^2 - \frac{405\delta\chi_a\chi_s}{4} - \left(\frac{405}{8} - \frac{5\eta}{2} \right) \chi_s^2, \\ \psi_{2.5\text{PN}}^{\text{PP}} &= \frac{38645\pi}{756} - \frac{65\pi\eta}{9} + \left(-\frac{732985}{2268} + \frac{24260}{81}\eta + \frac{340}{9}\eta^2 \right) \chi_s + \left(-\frac{732985}{2268}\delta - \frac{140}{9}\delta\eta \right) \chi_a, \\ \psi_{3\text{PN}}^{\text{PP}} &= \frac{11583231236531}{4694215680} - \frac{6848\gamma_E}{21} - \frac{640\pi^2}{3} - \left(\frac{15737765635}{3048192} - \frac{2255\pi^2}{12} \right) \eta + \frac{76055\eta^2}{1728} \\ & - \frac{127825\eta^3}{1296} + \frac{2270\pi\delta\chi_a}{3} + \left(\frac{75515}{288} - \frac{263245\eta}{252} - 480\eta^2 \right) \chi_a^2 \\ & + \left(\frac{2270\pi}{3} - 520\pi\eta + \left(\frac{75515\delta}{144} - \frac{8225\delta\eta}{18} \right) \chi_a \right) \chi_s \\ & + \left(\frac{75515}{288} - \frac{232415\eta}{504} + \frac{1255\eta^2}{9} \right) \chi_s^2 - \frac{13696 \ln 2}{21}, \end{aligned} \quad (\text{A.22})$$

$$\begin{aligned}
\psi_{3\text{PN}}^{\text{pp,ln}} &= -\frac{6848}{21}, \\
\psi_{3.5\text{PN}}^{\text{pp}} &= \frac{77096675\pi}{254016} + \frac{378515\pi\eta}{1512} - \frac{74045\pi\eta^2}{756} + \left(-\frac{25150083775\delta}{3048192} + \frac{26804935\delta\eta}{6048} - \frac{1985\delta\eta^2}{48} \right) \chi_a \\
&\quad + \left(-\frac{815\pi}{2} + 1600\pi\eta \right) \chi_a^2 + \left(\frac{14585\delta}{24} - 2380\delta\eta \right) \chi_a^3 \\
&\quad + \left(-\frac{25150083775}{3048192} + \frac{10566655595\eta}{762048} - \frac{1042165\eta^2}{3024} + \frac{5345\eta^3}{36} \right. \\
&\quad \left. - 815\pi\delta\chi_a + \left(\frac{14585}{8} - 7270\eta + 80\eta^2 \right) \chi_a^2 \right) \chi_s \\
&\quad + \left(-\frac{815\pi}{2} + 30\pi\eta + \left(\frac{14585\delta}{8} - \frac{215\delta\eta}{2} \right) \chi_a \right) \chi_s^2 + \left(\frac{14585}{24} - \frac{475\eta}{6} + \frac{100\eta^2}{3} \right) \chi_s^3, \\
\psi_{4\text{PN}}^{\text{pp}} &= -\frac{90490\pi^2}{567} - \frac{36812\gamma_E}{189} + \frac{2550713843998885153}{830425530654720} - \frac{26325 \ln 3}{196} - \frac{1011020 \ln 2}{3969} \\
&\quad + \eta \left(-\frac{680712846248317}{126743823360} - \frac{3911888\gamma_E}{3969} + \frac{109295\pi^2}{672} - \frac{9964112 \ln 2}{3969} + \frac{26325 \ln 3}{49} \right) \\
&\quad + \left(\frac{7510073635}{9144576} - \frac{11275\pi^2}{432} \right) \eta^2 + \frac{1292395\eta^3}{36288} - \frac{5975\eta^4}{288}, \\
\psi_{4\text{PN}}^{\text{pp,ln}^2} &= \frac{1955944\eta}{1323} + \frac{18406}{63}.
\end{aligned}$$

Note that the constant “1” terms in the $(1 \pm 3 \ln v)$ factors in (3.55) and (A.21) at 2.5PN and 4PN orders are occasionally ignored in the literature as they can be absorbed into the redefinition of ϕ_0 and t_0 respectively. On the other hand, the $\pm 3 \ln v$ terms cannot be absorbed into redefinitions and arise from integrations of the form $\int dv/v$ when computing $\phi(v)$ and $t(v)$ in (A.18). The presence of these logarithms is the reason why the 2.5PN and 4PN coefficients are still important in the PN waveform model.

Energy Loss

With the flux radiated to infinity given in Eq. (A.8) and the flux at the horizon in Eq. (A.16), we may also derive the analytic expression for the energy loss during the inspiral phase:

$$\Delta E_\infty(v) = \int \mathcal{F}_\infty \frac{dv}{\dot{v}}, \quad \Delta E_{\text{H}}(v) = \int \dot{M} \frac{dv}{\dot{v}}. \quad (\text{A.23})$$

In the above expression, \dot{v} is given in Eq. (A.19). Solving this iteratively, we get the energy loss at infinity

$$\begin{aligned}
\Delta E_\infty(v) &= \frac{1}{2} M v^2 \eta \left[1 + \Delta E_\infty^{1\text{PN}} v^2 + \Delta E_\infty^{1.5\text{PN}} v^3 + \Delta E_\infty^{2\text{PN}} v^4 + \Delta E_\infty^{2.5\text{PN}} v^5 \right. \\
&\quad \left. + \Delta E_\infty^{3\text{PN}} v^6 + \Delta E_\infty^{3.5\text{PN}} v^7 + \Delta E_\infty^{4\text{PN}} v^8 + \Delta E_\infty^{4\text{PN,ln}} v^8 \ln v \right], \quad (\text{A.24})
\end{aligned}$$

where

$$\begin{aligned}
\Delta E_\infty^{1\text{PN}} &= -\frac{3}{4} - \frac{\eta}{12}, \quad \Delta E_\infty^{1.5\text{PN}} = \frac{8}{3}\delta\chi_a + \frac{8}{3}\chi_s - \frac{4}{3}\eta\chi_s, \\
\Delta E_\infty^{2\text{PN}} &= -\frac{27}{8} + \frac{19}{8}\eta - \frac{\eta^2}{24} + (-1 + 4\eta)\chi_a^2 - 2\delta\chi_a\chi_s - \chi_s^2, \\
\Delta E_\infty^{2.5\text{PN}} &= \left(8\delta - \frac{31}{9}\delta\eta\right)\chi_a + \left(8 - \frac{121}{9}\eta + \frac{2}{9}\eta^2\right)\chi_s - \frac{45}{112}\bar{\mathcal{H}}_1^E\chi_a - \frac{45}{112}\mathcal{H}_1^E\chi_s, \\
\Delta E_\infty^{3\text{PN}} &= -\frac{675}{64} + \left(\frac{34445}{576} - \frac{205}{96}\pi^2\right)\eta - \frac{155}{96}\eta^2 - \frac{35}{5184}\eta^3 \\
&\quad + \left(-\frac{65}{18} + \frac{305}{18}\eta - \frac{10}{3}\eta^2\right)\chi_a^2 + \left(-\frac{65}{9}\delta + \frac{145}{9}\delta\eta\right)\chi_a\chi_s + \left(-\frac{65}{18} + \frac{245}{18}\eta - \frac{40}{9}\eta^2\right)\chi_s^2, \\
\Delta E_\infty^{3.5\text{PN}} &= \left(27\delta - \frac{211}{4}\delta\eta + \frac{7}{6}\delta\eta^2\right)\chi_a + \left(27 - \frac{373}{4}\eta + \frac{86}{3}\eta^2 + \frac{\eta^3}{6}\right)\chi_s + (-4\eta + 16\eta^2)\chi_a^2\chi_s \\
&\quad - 8\delta\eta\chi_a\chi_s^2 - 4\eta\chi_s^3 + \left(\left(-\frac{7495}{5376} - \frac{5}{64}\eta\right)\chi_a - \frac{15}{64}\delta\chi_s\right)\bar{\mathcal{H}}_1^E - \frac{5}{16}\chi_a\bar{\mathcal{H}}_1^B \\
&\quad + \left(\left(-\frac{7495}{5376} - \frac{5}{64}\eta\right)\chi_s - \frac{15}{64}\delta\chi_a\right)\mathcal{H}_1^E - \frac{5}{16}\chi_s\mathcal{H}_1^B, \\
\Delta E_\infty^{4\text{PN}} &= -\frac{3969}{128} + \eta\left(-\frac{123671}{5760} + \frac{896}{15}\gamma_E + \frac{9037}{1536}\pi^2 + \frac{1792}{15}\log(2)\right) + \left(-\frac{498449}{3456} + \frac{3157}{576}\pi^2\right)\eta^2 \\
&\quad + \frac{301}{1728}\eta^3 + \frac{77}{31104}\eta^4 - \frac{9}{16}\mathcal{H}_0, \\
\Delta E_\infty^{4\text{PN},\text{ln}} &= \frac{896}{15}.
\end{aligned} \tag{A.25}$$

The energy loss at the horizon is given by

$$\Delta E_{\text{H}}(v) = \frac{1}{2}Mv^2\eta\left[\Delta E_{\text{H}}^{2.5\text{PN}}v^5 + \Delta E_{\text{H}}^{3.5\text{PN}}v^7 + \Delta E_{\text{H}}^{4\text{PN}}v^8\right] \tag{A.26}$$

where

$$\begin{aligned}
\Delta E_{\text{H}}^{2.5\text{PN}} &= \frac{45}{112}\mathcal{H}_1^E\chi_s + \frac{45}{112}\bar{\mathcal{H}}_1^E\chi_a, \\
\Delta E_{\text{H}}^{3.5\text{PN}} &= \left(\frac{5}{16}\mathcal{H}_1^B + \frac{7915}{5376}\mathcal{H}_1^E + \frac{5}{32}\bar{\mathcal{H}}_1^E\delta - \frac{5}{64}\mathcal{H}_1^E\eta\right)\chi_s \\
&\quad + \left(\frac{5}{16}\bar{\mathcal{H}}_1^B + \frac{7915}{5376}\bar{\mathcal{H}}_1^E + \frac{5}{32}\mathcal{H}_1^E\delta - \frac{5}{64}\bar{\mathcal{H}}_1^E\eta\right)\chi_a, \\
\Delta E_{\text{H}}^{4\text{PN}} &= \frac{9}{16}\mathcal{H}_0.
\end{aligned} \tag{A.27}$$

GW Amplitude

In the stationary phase approximation [142], the Fourier domain waveform amplitude defined in (3.50) takes the form [139, 144, 165]

$$A(v) = \frac{2\eta M}{D}v^2\left(\dot{F}(v)\right)_{F=f}^{-1/2}, \tag{A.28}$$

where $(\dot{F}(v))_{F=f}$ is the time derivative of the instantaneous GW frequency evaluated at the stationary point, $F = f = v^3/(\pi M)$. Using chain rule and the energy balance equation (A.17),

one can re-express the instantaneous frequency derivative and the amplitude as

$$\dot{F}(v) = \frac{\partial F}{\partial v} \frac{\partial v}{\partial \mathcal{E}} \dot{\mathcal{E}}, \quad A(v) = \frac{2\eta M^{3/2} v}{D} \sqrt{\frac{\pi}{3}} \left[\frac{-\partial \mathcal{E} / \partial v}{\mathcal{F}_\infty + \dot{M}} \right]^{1/2}, \quad (\text{A.29})$$

Substituting (A.3), (A.8) and (A.16) for the binding energy and fluxes, one obtains

$$A(f) = \sqrt{\frac{5}{24}} \frac{\mathcal{M}^{5/6}}{D \pi^{2/3}} f^{-7/6} \left[A^{\text{PP}}(f) + A^{\text{TDN}}(f) \right], \quad (\text{A.30})$$

where the amplitude corrections from tidal dissipation effects are shown in (3.59) and (3.60), while the point particle contributions are

$$A^{\text{PP}}(f) = 1 + v^2 A_{1\text{PN}}^{\text{PP}} + v^3 A_{1.5\text{PN}}^{\text{PP}} + v^4 A_{2\text{PN}}^{\text{PP}} + v^5 A_{2.5\text{PN}}^{\text{PP}} + v^6 A_{3\text{PN}}^{\text{PP}} + v^6 \ln v A_{3\text{PN}}^{\text{PP,ln}} + v^7 A_{3.5\text{PN}}^{\text{PP}} + v^8 A_{4\text{PN}}^{\text{PP}} + v^8 \ln v A_{4\text{PN}}^{\text{PP,ln}}, \quad (\text{A.31})$$

with the PN coefficients

$$\begin{aligned} A_{1\text{PN}}^{\text{PP}} &= \frac{11}{8}\eta + \frac{743}{672} \\ A_{1.5\text{PN}}^{\text{PP}} &= -2\pi + \frac{113}{24}\delta\chi_a + \frac{113}{24}\chi_s - \frac{19}{6}\eta\chi_s \\ A_{2\text{PN}}^{\text{PP}} &= \frac{7266251}{8128512} + \frac{18913\eta}{16128} + \frac{1379\eta^2}{1152} - \left(\frac{81}{32} - 10\eta\right)\chi_a^2 - \frac{81\delta\chi_a\chi_s}{16} - \left(\frac{81}{32} - \frac{\eta}{8}\right)\chi_s^2, \\ A_{2.5\text{PN}}^{\text{PP}} &= -\frac{4757\pi}{1344} + \frac{57\pi\eta}{16} + \left(\frac{502429\delta}{16128} - \frac{907\delta\eta}{192}\right)\chi_a + \left(\frac{502429}{16128} - \frac{73921\eta}{2016} + \frac{5\eta^2}{48}\right)\chi_s, \\ A_{3\text{PN}}^{\text{PP}} &= -\frac{29342493702821}{500716339200} + \frac{856\gamma_E}{105} + \frac{10\pi^2}{3} + \frac{1712 \ln 2}{105} + \left(\frac{3526813753}{27869184} - \frac{451\pi^2}{96}\right)\eta \\ &\quad - \frac{1041557\eta^2}{258048} + \frac{67999\eta^3}{82944} - \frac{19\pi\delta\chi_a}{2} + \left(-\frac{19\pi}{2} + \frac{20\pi\eta}{3}\right)\chi_s \\ &\quad + \left(-\frac{319133}{21504} + \frac{48289\eta}{768} - \frac{7\eta^2}{4}\right)\chi_a^2 + \left(-\frac{319133\delta}{10752} + \frac{12785\delta\eta}{384}\right)\chi_a\chi_s \\ &\quad + \left(-\frac{319133}{21504} + \frac{40025\eta}{1344} - \frac{555\eta^2}{64}\right)\chi_s^2, \\ A_{3\text{PN}}^{\text{PP,ln}} &= \frac{856}{105}, \\ A_{3.5\text{PN}}^{\text{PP}} &= -\frac{5111593\pi}{2709504} - \frac{72221\pi\eta}{24192} - \frac{1349\pi\eta^2}{24192} + \left(\frac{1557122011\delta}{9289728} - \frac{2206797\delta\eta}{14336} + \frac{52343\delta\eta^2}{27648}\right)\chi_a \\ &\quad + \left(\frac{41\pi}{8} - 20\pi\eta\right)\chi_a^2 + \left(-\frac{2515\delta}{768} + \frac{149\delta\eta}{12}\right)\chi_a^3 + \left[\frac{1557122011}{9289728} - \frac{1905526039\eta}{5419008}\right. \\ &\quad \left. + \frac{11030651\eta^2}{193536} - \frac{445\eta^3}{6912} + \frac{41\pi\delta\chi_a}{4} + \left(-\frac{2515}{256} + \frac{6011\eta}{192} + \frac{89\eta^2}{3}\right)\chi_a^2\right]\chi_s \\ &\quad + \left(\frac{41\pi}{8} - \frac{\pi\eta}{2} + \left(-\frac{2515\delta}{256} - \frac{2675\delta\eta}{192}\right)\chi_a\right)\chi_s^2 - \left(\frac{2515}{768} + \frac{53\eta}{8} + \frac{7\eta^2}{16}\right)\chi_s^3, \\ A_{4\text{PN}}^{\text{PP}} &= -\frac{246427872050556151}{899847347503104} + \frac{56881\gamma_E}{4410} + \frac{14495\pi^2}{2016} + \left(-\frac{2469217875055}{9364045824} + \frac{451\pi^2}{48}\right)\eta^2 \end{aligned} \quad (\text{A.32})$$

$$\begin{aligned}
& -\frac{42749765\eta^3}{55738368} + \frac{144587\eta^4}{294912} + \frac{10417\ln 2}{980} + \frac{47385\ln 3}{3136} \\
& + \eta \left(\frac{997052025430343}{1716741734400} + \frac{219776\gamma_E}{2205} - \frac{681325\pi^2}{64512} + \frac{573323\ln 2}{2205} - \frac{47385\ln 3}{784} \right), \\
A_{4\text{PN}}^{\text{pp,ln}} = & \left(\frac{56881}{4410} + \frac{219776}{2205}\eta \right).
\end{aligned}$$

References

- [1] B. Abbott *et al.* (LIGO/Virgo Collaboration), “GWTC-1: A Gravitational-Wave Transient Catalog of Compact Binary Mergers Observed by LIGO and Virgo during the First and Second Observing Runs,” *Phys. Rev.* **X9** (2019) 031040, [arXiv:1811.12907](#) [[astro-ph.HE](#)].
- [2] **LIGO Scientific, Virgo** Collaboration, R. Abbott *et al.*, “GWTC-2: Compact Binary Coalescences Observed by LIGO and Virgo During the First Half of the Third Observing Run,” *Phys. Rev. X* **11** (2021) 021053, [arXiv:2010.14527](#) [[gr-qc](#)].
- [3] **LIGO Scientific, VIRGO** Collaboration, R. Abbott *et al.*, “GWTC-2.1: Deep Extended Catalog of Compact Binary Coalescences Observed by LIGO and Virgo During the First Half of the Third Observing Run,” [arXiv:2108.01045](#) [[gr-qc](#)].
- [4] **LIGO Scientific, VIRGO, KAGRA** Collaboration, R. Abbott *et al.*, “GWTC-3: Compact Binary Coalescences Observed by LIGO and Virgo During the Second Part of the Third Observing Run,” [arXiv:2111.03606](#) [[gr-qc](#)].
- [5] T. Venumadhav, B. Zackay, J. Roulet, L. Dai, and M. Zaldarriaga, “New Search Pipeline for Compact Binary Mergers: Results for Binary Black Holes in the First Observing Run of Advanced LIGO,” *Phys. Rev.* **D100** (2019) 023011, [arXiv:1902.10341](#) [[astro-ph.IM](#)].
- [6] T. Venumadhav, B. Zackay, J. Roulet, L. Dai, and M. Zaldarriaga, “New Binary Black Hole Mergers in the Second Observing Run of Advanced LIGO and Advanced Virgo,” *Phys. Rev. D* **101** (2020) 083030, [arXiv:1904.07214](#) [[astro-ph.HE](#)].
- [7] S. Olsen, T. Venumadhav, J. Mushkin, J. Roulet, B. Zackay, and M. Zaldarriaga, “New binary black hole mergers in the LIGO-Virgo O3a data,” *Phys. Rev. D* **106** no. 4, (2022) 043009, [arXiv:2201.02252](#) [[astro-ph.HE](#)].
- [8] A. H. Nitz, C. Capano, A. B. Nielsen, S. Reyes, R. White, D. A. Brown, and B. Krishnan, “1-OGC: The first open gravitational-wave catalog of binary mergers from analysis of public Advanced LIGO data,” *Astrophys. J.* **872** no. 2, (2019) 195, [arXiv:1811.01921](#) [[gr-qc](#)].
- [9] A. H. Nitz, T. Dent, G. S. Davies, S. Kumar, C. D. Capano, I. Harry, S. Mozzon, L. Nuttall, A. Lundgren, and M. Tápai, “2-OGC: Open Gravitational-wave Catalog of Binary Mergers from Analysis of Public Advanced LIGO and Virgo Data,” *Astrophys. J.* **891** (10, 2019) 123, [arXiv:1910.05331](#) [[astro-ph.HE](#)].
- [10] A. H. Nitz, C. D. Capano, S. Kumar, Y.-F. Wang, S. Kastha, M. Schäfer, R. Dhurkunde, and M. Cabero, “3-OGC: Catalog of Gravitational Waves from Compact-binary Mergers,” *Astrophys. J.* **922** no. 1, (2021) 76, [arXiv:2105.09151](#) [[astro-ph.HE](#)].
- [11] A. H. Nitz, S. Kumar, Y.-F. Wang, S. Kastha, S. Wu, M. Schäfer, R. Dhurkunde, and C. D. Capano, “4-OGC: Catalog of Gravitational Waves from Compact Binary Mergers,” *Astrophys. J.* **946** no. 2, (2023) 59, [arXiv:2112.06878](#) [[astro-ph.HE](#)].
- [12] H. S. Chia, T. D. P. Edwards, D. Wadekar, A. Zimmerman, S. Olsen, J. Roulet, T. Venumadhav,

- B. Zackay, and M. Zaldarriaga, “In Pursuit of Love: First Templated Search for Compact Objects with Large Tidal Deformabilities in the LIGO-Virgo Data,” [arXiv:2306.00050](#) [[gr-qc](#)].
- [13] A. K. Mehta, S. Olsen, D. Wadekar, J. Roulet, T. Venumadhav, J. Mushkin, B. Zackay, and M. Zaldarriaga, “New binary black hole mergers in the LIGO-Virgo O3b data,” [arXiv:2311.06061](#) [[gr-qc](#)].
- [14] D. Wadekar, J. Roulet, T. Venumadhav, A. K. Mehta, B. Zackay, J. Mushkin, S. Olsen, and M. Zaldarriaga, “New black hole mergers in the LIGO-Virgo O3 data from a gravitational wave search including higher-order harmonics,” [arXiv:2312.06631](#) [[gr-qc](#)].
- [15] L. Blanchet, “Gravitational Radiation from Post-Newtonian Sources and Inspiralling Compact Binaries,” *Living Rev. Rel.* **17** (2014) 2, [arXiv:1310.1528](#) [[gr-qc](#)].
- [16] J. Blümlein, A. Maier, P. Marquard, and G. Schäfer, “The fifth-order post-Newtonian Hamiltonian dynamics of two-body systems from an effective field theory approach,” *Nucl. Phys. B* **983** (2022) 115900, [arXiv:2110.13822](#) [[gr-qc](#)]. [Erratum: *Nucl.Phys.B* 985, 115991 (2022)].
- [17] J. Blümlein, A. Maier, P. Marquard, and G. Schäfer, “The 6th post-Newtonian potential terms at $O(G_N^4)$,” *Phys. Lett. B* **816** (2021) 136260, [arXiv:2101.08630](#) [[gr-qc](#)].
- [18] G. Cho, R. A. Porto, and Z. Yang, “Gravitational radiation from inspiralling compact objects: Spin effects to the fourth post-Newtonian order,” *Phys. Rev. D* **106** no. 10, (2022) L101501, [arXiv:2201.05138](#) [[gr-qc](#)].
- [19] L. Blanchet, G. Faye, Q. Henry, F. Larrouturou, and D. Trestini, “Gravitational waves from compact binaries to the fourth post-Newtonian order,” in *57th Rencontres de Moriond on Gravitation*. 4, 2023. [arXiv:2304.13647](#) [[gr-qc](#)].
- [20] D. Trestini and L. Blanchet, “Gravitational-wave tails of memory at 4PN order,” in *57th Rencontres de Moriond on Gravitation*. 6, 2023. [arXiv:2306.00546](#) [[gr-qc](#)].
- [21] E. Poisson, “Gravitational Waves from Inspirling Compact Binaries: The Quadrupole Moment Term,” *Phys. Rev. D* **57** (1998) 5287, [arXiv:gr-qc/9709032](#) [[gr-qc](#)].
- [22] R. A. Porto, “Post-Newtonian corrections to the motion of spinning bodies in NRGR,” *Phys. Rev. D* **73** (2006) 104031, [arXiv:gr-qc/0511061](#).
- [23] S. Marsat, “Cubic Order Spin Effects in the Dynamics and Gravitational Wave Energy Flux of Compact Object Binaries,” *Class. Quant. Grav.* **32** (2015) 085008, [arXiv:1411.4118](#) [[gr-qc](#)].
- [24] M. Levi and J. Steinhoff, “Leading Order Finite Size Effects with Spins for Inspiralling Compact Binaries,” *JHEP* **06** (2015) 059, [arXiv:1410.2601](#) [[gr-qc](#)].
- [25] M. Levi and J. Steinhoff, “Spinning gravitating objects in the effective field theory in the post-Newtonian scheme,” *JHEP* **09** (2015) 219, [arXiv:1501.04956](#) [[gr-qc](#)].
- [26] N. Krishnendu, K. Arun, and C. Mishra, “Testing the Binary Black Hole Nature of a Compact Binary Coalescence,” *Phys. Rev. Lett.* **119** (2017) 091101, [arXiv:1701.06318](#) [[gr-qc](#)].
- [27] N. V. Krishnendu, C. K. Mishra, and K. G. Arun, “Spin-Induced Deformations and Tests of Binary Black Hole Nature Using Third-Generation Detectors,” *Phys. Rev.* **D99** (2019) 064008, [arXiv:1811.00317](#) [[gr-qc](#)].
- [28] H. S. Chia and T. D. Edwards, “Searching for General Binary Inspirals with Gravitational Waves,” *JCAP* **11** (2020) 033, [arXiv:2004.06729](#) [[astro-ph.HE](#)].
- [29] H. S. Chia, T. D. P. Edwards, R. N. George, A. Zimmerman, A. Coogan, K. Freese, C. Messick, and C. N. Setzer, “Dimensionally Reduced Waveforms for Spin-Induced Quadrupole Searches,” [arXiv:2211.00039](#) [[gr-qc](#)].

- [30] Z. Lyu, M. LaHaye, H. Yang, and B. Bonga, “Probing spin-induced quadrupole moments in precessing compact binaries,” *Phys. Rev. D* **109** no. 6, (2024) 064081, [arXiv:2308.09032 \[gr-qc\]](#).
- [31] H. Love, “Some problems of geodynamics,” *Nature* **89** no. 2228, (1912) 471–472. <https://doi.org/10.1038/089471a0>.
- [32] W. D. Goldberger and I. Z. Rothstein, “An Effective field theory of gravity for extended objects,” *Phys. Rev. D* **73** (2006) 104029, [arXiv:hep-th/0409156](#).
- [33] E. Flanagan and T. Hinderer, “Constraining Neutron Star Tidal Love Numbers with Gravitational Wave Detectors,” *Phys. Rev. D* **77** (2008) 021502, [arXiv:0709.1915 \[astro-ph\]](#).
- [34] C. Li and G. Lovelace, “A Generalization of Ryan’s theorem: Probing tidal coupling with gravitational waves from nearly circular, nearly equatorial, extreme-mass-ratio inspirals,” *Phys. Rev. D* **77** (2008) 064022, [arXiv:gr-qc/0702146](#).
- [35] T. Damour and A. Nagar, “Relativistic Tidal Properties of Neutron Stars,” *Phys. Rev. D* **80** (2009) 084035, [arXiv:0906.0096 \[gr-qc\]](#).
- [36] T. Binnington and E. Poisson, “Relativistic Theory of Tidal Love Numbers,” *Phys. Rev. D* **80** (2009) 084018, [arXiv:0906.1366 \[gr-qc\]](#).
- [37] J. Vines, E. E. Flanagan, and T. Hinderer, “Post-1-Newtonian Tidal Effects in the Gravitational Waveform from Binary Inspirals,” *Phys. Rev. D* **83** (2011) 084051, [arXiv:1101.1673 \[gr-qc\]](#).
- [38] V. Cardoso, E. Franzin, A. Maselli, P. Pani, and G. Raposo, “Testing Strong-Field Gravity with Tidal Love Numbers,” *Phys. Rev. D* **95** (2017) 084014, [arXiv:1701.01116 \[gr-qc\]](#). [Addendum: *Phys. Rev. D* **95** (2017) 089901].
- [39] J. B. Hartle, “Tidal friction in slowly rotating black holes,” *Phys. Rev. D* **8** (Aug, 1973) 1010–1024. <https://link.aps.org/doi/10.1103/PhysRevD.8.1010>.
- [40] E. Poisson and M. Sasaki, “Gravitational radiation from a particle in circular orbit around a black hole. 5: Black hole absorption and tail corrections,” *Phys. Rev. D* **51** (1995) 5753–5767, [arXiv:gr-qc/9412027](#).
- [41] H. Tagoshi, S. Mano, and E. Takasugi, “PostNewtonian expansion of gravitational waves from a particle in circular orbits around a rotating black hole: Effects of black hole absorption,” *Prog. Theor. Phys.* **98** (1997) 829–850, [arXiv:gr-qc/9711072](#).
- [42] K. Alvi, “Energy and angular momentum flow into a black hole in a binary,” *Phys. Rev. D* **64** (2001) 104020, [arXiv:gr-qc/0107080](#).
- [43] S. A. Hughes, “Evolution of circular, nonequatorial orbits of Kerr black holes due to gravitational wave emission. II. Inspiral trajectories and gravitational wave forms,” *Phys. Rev. D* **64** (2001) 064004, [arXiv:gr-qc/0104041](#). [Erratum: *Phys.Rev.D* **88**, 109902 (2013)].
- [44] E. Poisson, “Tidal interaction of black holes and Newtonian viscous bodies,” *Phys. Rev. D* **80** (2009) 064029, [arXiv:0907.0874 \[gr-qc\]](#).
- [45] J.-P. Zahn, “Tidal dissipation in binary systems,” *EAS Publ. Ser.* **29** (2008) 67, [arXiv:0807.4870 \[astro-ph\]](#).
- [46] G. I. Ogilvie, “Tidal dissipation in stars and giant planets,” *Ann. Rev. Astron. Astrophys.* **52** (2014) 171–210, [arXiv:1406.2207 \[astro-ph.SR\]](#).
- [47] E. Poisson and C. M. Will, *Gravity: Newtonian, Post-Newtonian, Relativistic*. Cambridge University Press, 2014.
- [48] C. D. Murray and S. F. Dermott, *Solar system dynamics*. Cambridge university press, 1999.

- [49] S. Endlich and R. Penco, “Effective field theory approach to tidal dynamics of spinning astrophysical systems,” *Phys. Rev. D* **93** no. 6, (2016) 064021, [arXiv:1510.08889](#) [gr-qc].
- [50] J. P. Zahn, “Tidal friction in close binary systems,” *Astronomy and Astrophysics* **57** (May, 1977) 383–394.
- [51] S. E. de Mink, M. Cantiello, N. Langer, O. R. Pols, I. Brott, and S. C. Yoon, “Rotational mixing in massive binaries. Detached short-period systems,” *Astronomy and Astrophysics* **497** no. 1, (Apr., 2009) 243–253, [arXiv:0902.1751](#) [astro-ph.SR].
- [52] M. Zaldarriaga, D. Kushnir, and J. A. Kollmeier, “The expected spins of gravitational wave sources with isolated field binary progenitors,” *Mon. Not. Roy. Astron. Soc.* **473** no. 3, (2018) 4174–4178, [arXiv:1702.00885](#) [astro-ph.HE].
- [53] A. Olejak and K. Belczynski, “The Implications of High BH Spins on the Origin of BH–BH Mergers,” *Astrophys. J. Lett.* **921** no. 1, (2021) L2, [arXiv:2109.06872](#) [astro-ph.HE].
- [54] L. Ma and J. Fuller, “Tidal Spin-up of Black Hole Progenitor Stars,” *Astrophys. J.* **952** no. 1, (2023) 53, [arXiv:2305.08356](#) [astro-ph.HE].
- [55] B. Zackay, T. Venumadhav, L. Dai, J. Roulet, and M. Zaldarriaga, “Highly Spinning and Aligned Binary Black Hole Merger in the Advanced LIGO First Observing Run,” *Phys. Rev. D* **100** (2019) 023007, [arXiv:1902.10331](#) [astro-ph.HE].
- [56] **LIGO Scientific, Virgo** Collaboration, R. Abbott *et al.*, “Population Properties of Compact Objects from the Second LIGO-Virgo Gravitational-Wave Transient Catalog,” *Astrophys. J. Lett.* **913** no. 1, (2021) L7, [arXiv:2010.14533](#) [astro-ph.HE].
- [57] H. S. Chia, S. Olsen, J. Roulet, L. Dai, T. Venumadhav, B. Zackay, and M. Zaldarriaga, “Signs of higher multipoles and orbital precession in GW151226,” *Phys. Rev. D* **106** no. 2, (2022) 024009, [arXiv:2105.06486](#) [astro-ph.HE].
- [58] J. Roulet, H. S. Chia, S. Olsen, L. Dai, T. Venumadhav, B. Zackay, and M. Zaldarriaga, “Distribution of effective spins and masses of binary black holes from the LIGO and Virgo O1–O3a observing runs,” *Phys. Rev. D* **104** no. 8, (2021) 083010, [arXiv:2105.10580](#) [astro-ph.HE].
- [59] **KAGRA, VIRGO, LIGO Scientific** Collaboration, R. Abbott *et al.*, “Population of Merging Compact Binaries Inferred Using Gravitational Waves through GWTC-3,” *Phys. Rev. X* **13** no. 1, (2023) 011048, [arXiv:2111.03634](#) [astro-ph.HE].
- [60] Y. B. Zel’Dovich, “Generation of waves by a rotating body,” *Soviet Journal of Experimental and Theoretical Physics Letters* **14** (1971) 180.
- [61] Y. Zel’Dovich, “Amplification of Cylindrical Electromagnetic Waves Reflected from a Rotating Body,” *Sov. Phys. JETP* **35** (1972) 1085.
- [62] A. A. Starobinskil and S. M. Churilov, “Amplification of electromagnetic and gravitational waves scattered by a rotating ”black hole”,” *Sov. Phys. JETP* **65** no. 1, (1974) 1–5.
- [63] A. Starobinsky, “Amplification of Waves Reflected from a Rotating “Black Hole”,” *Sov. Phys. JETP* **37** (1973) 28. [*Zh. Eksp. Teor. Fiz.* **64** (1973) 48].
- [64] S. Detweiler, “Klein-Gordon Equation and Rotating Black Holes,” *Phys. Rev.* **D22** (1980) 2323–2326.
- [65] J. D. Bekenstein and M. Schiffer, “The Many Faces of Superradiance,” *Phys. Rev.* **D58** (1998) 064014, [arXiv:gr-qc/9803033](#) [gr-qc].
- [66] S. Dolan, “Instability of the Massive Klein-Gordon Field on the Kerr Spacetime,” *Phys. Rev.* **D76** (2007) 084001, [arXiv:0705.2880](#) [gr-qc].

- [67] R. Brito, V. Cardoso, and P. Pani, “Superradiance,” *Lect. Notes Phys.* **906** (2015) 1, [arXiv:1501.06570 \[gr-qc\]](#).
- [68] A. Arvanitaki, S. Dimopoulos, S. Dubovsky, N. Kaloper, and J. March-Russell, “String Axiverse,” *Phys. Rev. D* **81** (2010) 123530, [arXiv:0905.4720 \[hep-th\]](#).
- [69] A. Arvanitaki and S. Dubovsky, “Exploring the String Axiverse with Precision Black Hole Physics,” *Phys. Rev. D* **83** (2011) 044026, [arXiv:1004.3558 \[hep-th\]](#).
- [70] H. Witek, V. Cardoso, A. Ishibashi, and U. Sperhake, “Superradiant Instabilities in Astrophysical Systems,” *Phys. Rev. D* **87** (2013) 043513, [arXiv:1212.0551 \[gr-qc\]](#).
- [71] R. Brito, V. Cardoso, and P. Pani, “Black Holes as Particle Detectors: Evolution of Superradiant Instabilities,” *Class. Quant. Grav.* **32** (2015) 134001, [arXiv:1411.0686 \[gr-qc\]](#).
- [72] W. East and F. Pretorius, “Superradiant Instability and Backreaction of Massive Vector Fields around Kerr Black Holes,” *Phys. Rev. Lett.* **119** (2017) 041101, [arXiv:1704.04791 \[gr-qc\]](#).
- [73] D. Baumann, H. S. Chia, J. Stout, and L. ter Haar, “The Spectra of Gravitational Atoms,” *JCAP* **12** (2019) 006, [arXiv:1908.10370 \[gr-qc\]](#).
- [74] H. S. Chia, C. Doorman, A. Wernersson, T. Hinderer, and S. Nissanke, “Self-interacting gravitational atoms in the strong-gravity regime,” *JCAP* **04** (2023) 018, [arXiv:2212.11948 \[gr-qc\]](#).
- [75] H. Yoshino and H. Kodama, “Bosenova Collapse of Axion Cloud around a Rotating Black Hole,” *Prog. Theor. Phys.* **128** (2012) 153–190, [arXiv:1203.5070 \[gr-qc\]](#).
- [76] H. Yoshino and H. Kodama, “Gravitational Radiation from an Axion Cloud around a Black Hole: Superradiant Phase,” *PTEP* **2014** (2014) 043E02, [arXiv:1312.2326 \[gr-qc\]](#).
- [77] M. Baryakhtar, R. Lasenby, and M. Teo, “Black Hole Superradiance Signatures of Ultralight Vectors,” *Phys. Rev. D* **96** (2017) 035019, [arXiv:1704.05081 \[hep-ph\]](#).
- [78] D. Baumann, H. S. Chia, and R. A. Porto, “Probing Ultralight Bosons with Binary Black Holes,” *Phys. Rev. D* **99** (2019) 044001, [arXiv:1804.03208 \[gr-qc\]](#).
- [79] D. Baumann, H. S. Chia, R. A. Porto, and J. Stout, “Gravitational Collider Physics,” *Phys. Rev. D* **101** (2020) 083019, [arXiv:1912.04932 \[gr-qc\]](#).
- [80] H. S. Chia, *Probing Particle Physics with Gravitational Waves*. PhD thesis, Amsterdam U., 2020. [arXiv:2012.09167 \[hep-ph\]](#).
- [81] M. Baryakhtar, M. Galanis, R. Lasenby, and O. Simon, “Black hole superradiance of self-interacting scalar fields,” *Phys. Rev. D* **103** no. 9, (2021) 095019, [arXiv:2011.11646 \[hep-ph\]](#).
- [82] N. Siemonsen, C. Mondino, D. Egana-Ugrinovic, J. Huang, M. Baryakhtar, and W. E. East, “Dark photon superradiance: Electrodynamics and multimessenger signals,” *Phys. Rev. D* **107** no. 7, (2023) 075025, [arXiv:2212.09772 \[astro-ph.HE\]](#).
- [83] D. Baumann, G. Bertone, J. Stout, and G. M. Tomaselli, “Ionization of gravitational atoms,” *Phys. Rev. D* **105** no. 11, (2022) 115036, [arXiv:2112.14777 \[gr-qc\]](#).
- [84] G. M. Tomaselli, T. F. M. Spieksma, and G. Bertone, “The resonant history of gravitational atoms in black hole binaries,” [arXiv:2403.03147 \[gr-qc\]](#).
- [85] F. Ryan, “Gravitational Waves from the Inspiral of a Compact Object into a Massive, Axisymmetric Body with Arbitrary Multipole Moments,” *Phys. Rev. D* **52** (1995) 5707–5718.
- [86] S. Datta and S. Bose, “Probing the nature of central objects in extreme-mass-ratio inspirals with

- gravitational waves,” *Phys. Rev. D* **99** no. 8, (2019) 084001, [arXiv:1902.01723 \[gr-qc\]](#).
- [87] S. Datta, R. Brito, S. Bose, P. Pani, and S. A. Hughes, “Tidal heating as a discriminator for horizons in extreme mass ratio inspirals,” *Phys. Rev. D* **101** no. 4, (2020) 044004, [arXiv:1910.07841 \[gr-qc\]](#).
- [88] V. Cardoso and P. Pani, “Testing the Nature of Dark Compact Objects: a Status Report,” *Living Rev. Rel.* **22** (2019) , [arXiv:1904.05363 \[gr-qc\]](#).
- [89] J. L. Ripley, A. Hegade K. R., and N. Yunes, “Probing internal dissipative processes of neutron stars with gravitational waves during the inspiral of neutron star binaries,” [arXiv:2306.15633 \[gr-qc\]](#).
- [90] A. Maselli, P. Pani, V. Cardoso, T. Abdelsalhin, L. Gualtieri, and V. Ferrari, “Probing Planckian Corrections at the Horizon Scale with LISA Binaries,” *Phys. Rev. Lett.* **120** (2018) 081101, [arXiv:1703.10612 \[gr-qc\]](#).
- [91] S. Datta, K. S. Phukon, and S. Bose, “Recognizing black holes in gravitational-wave observations: Challenges in telling apart impostors in mass-gap binaries,” *Phys. Rev. D* **104** no. 8, (2021) 084006, [arXiv:2004.05974 \[gr-qc\]](#).
- [92] S. Datta, R. Brito, S. A. Hughes, T. Klinger, and P. Pani, “Tidal heating as a discriminator for horizons in equatorial eccentric extreme mass ratio inspirals,” [arXiv:2404.04013 \[gr-qc\]](#).
- [93] J. L. Ripley, A. Hegade K. R., R. S. Chandramouli, Yunes, and Nicolas, “First constraint on the dissipative tidal deformability of neutron stars,” [arXiv:2312.11659 \[gr-qc\]](#).
- [94] W. D. Goldberger and I. Z. Rothstein, “Dissipative effects in the worldline approach to black hole dynamics,” *Phys. Rev. D* **73** (2006) 104030, [arXiv:hep-th/0511133](#).
- [95] R. A. Porto, “Absorption effects due to spin in the worldline approach to black hole dynamics,” *Phys. Rev. D* **77** (2008) 064026, [arXiv:0710.5150 \[hep-th\]](#).
- [96] W. D. Goldberger, J. Li, and I. Z. Rothstein, “Non-conservative effects on spinning black holes from world-line effective field theory,” *JHEP* **06** (2021) 053, [arXiv:2012.14869 \[hep-th\]](#).
- [97] P. Charalambous, S. Dubovsky, and M. M. Ivanov, “On the Vanishing of Love Numbers for Kerr Black Holes,” *JHEP* **05** (2021) 038, [arXiv:2102.08917 \[hep-th\]](#).
- [98] M. M. Ivanov and Z. Zhou, “Black Hole Tidal Love Numbers and Dissipation Numbers in Worldline Effective Field Theory,” [arXiv:2208.08459 \[hep-th\]](#).
- [99] M. M. Ivanov and Z. Zhou, “Vanishing of Black Hole Tidal Love Numbers from Scattering Amplitudes,” *Phys. Rev. Lett.* **130** no. 9, (2023) 091403, [arXiv:2209.14324 \[hep-th\]](#).
- [100] M. V. S. Saketh, J. Steinhoff, J. Vines, and A. Buonanno, “Modeling horizon absorption in spinning binary black holes using effective worldline theory,” [arXiv:2212.13095 \[gr-qc\]](#).
- [101] R. A. Porto, “The effective field theorist’s approach to gravitational dynamics,” *Phys. Rept.* **633** (2016) 1–104, [arXiv:1601.04914 \[hep-th\]](#).
- [102] M. Levi, “Effective Field Theories of Post-Newtonian Gravity: A Comprehensive Review,” *Rept. Prog. Phys.* **83** (2020) 075901, [arXiv:1807.01699 \[hep-th\]](#).
- [103] W. D. Goldberger, “Effective field theories of gravity and compact binary dynamics: A Snowmass 2021 whitepaper,” in *2022 Snowmass Summer Study*. 6, 2022. [arXiv:2206.14249 \[hep-th\]](#).
- [104] W. D. Goldberger, “Effective Field Theory for Compact Binary Dynamics,” [arXiv:2212.06677 \[hep-th\]](#).
- [105] M. Favata, “Systematic parameter errors in inspiraling neutron star binaries,” *Phys. Rev. Lett.*

- 112 (2014) 101101, [arXiv:1310.8288 \[gr-qc\]](#).
- [106] B. Kol and M. Smolkin, “Black Hole Stereotyping: Induced Gravitational Static Polarization,” *JHEP* **02** (2012) 010, [arXiv:1110.3764 \[hep-th\]](#).
- [107] L. Hui, A. Joyce, R. Penco, L. Santoni, and A. R. Solomon, “Static response and Love numbers of Schwarzschild black holes,” *JCAP* **04** (2021) 052, [arXiv:2010.00593 \[hep-th\]](#).
- [108] A. Le Tiec and M. Casals, “Spinning Black Holes Fall in Love,” *Phys. Rev. Lett.* **126** no. 13, (2021) 131102, [arXiv:2007.00214 \[gr-qc\]](#).
- [109] H. S. Chia, “Tidal Deformation and Dissipation of Rotating Black Holes,” [arXiv:2010.07300 \[gr-qc\]](#).
- [110] P. Charalambous, S. Dubovsky, and M. M. Ivanov, “Hidden Symmetry of Vanishing Love Numbers,” *Phys. Rev. Lett.* **127** no. 10, (2021) 101101, [arXiv:2103.01234 \[hep-th\]](#).
- [111] L. Hui, A. Joyce, R. Penco, L. Santoni, and A. R. Solomon, “Ladder symmetries of black holes. Implications for love numbers and no-hair theorems,” *JCAP* **01** no. 01, (2022) 032, [arXiv:2105.01069 \[hep-th\]](#).
- [112] P. Charalambous, S. Dubovsky, and M. M. Ivanov, “Love symmetry,” *JHEP* **10** (2022) 175, [arXiv:2209.02091 \[hep-th\]](#).
- [113] L. Hui, A. Joyce, R. Penco, L. Santoni, and A. R. Solomon, “Near-zone symmetries of Kerr black holes,” *JHEP* **09** (2022) 049, [arXiv:2203.08832 \[hep-th\]](#).
- [114] V. De Luca, J. Khoury, and S. S. C. Wong, “Implications of the weak gravity conjecture for tidal Love numbers of black holes,” *Phys. Rev. D* **108** no. 4, (2023) 044066, [arXiv:2211.14325 \[hep-th\]](#).
- [115] P. Charalambous and M. M. Ivanov, “Scalar Love numbers and Love symmetries of 5-dimensional Myers-Perry black holes,” *JHEP* **07** (2023) 222, [arXiv:2303.16036 \[hep-th\]](#).
- [116] M. J. Rodriguez, L. Santoni, A. R. Solomon, and L. F. Temoche, “Love numbers for rotating black holes in higher dimensions,” *Phys. Rev. D* **108** no. 8, (2023) 084011, [arXiv:2304.03743 \[hep-th\]](#).
- [117] V. De Luca, J. Khoury, and S. S. C. Wong, “Nonlinearities in the tidal Love numbers of black holes,” *Phys. Rev. D* **108** no. 2, (2023) 024048, [arXiv:2305.14444 \[gr-qc\]](#).
- [118] P. Charalambous, “Love numbers and Love symmetries for p -form and gravitational perturbations of higher-dimensional spherically symmetric black holes,” [arXiv:2402.07574 \[hep-th\]](#).
- [119] E. Berti, V. De Luca, L. Del Grosso, and P. Pani, “Tidal Love numbers and approximate universal relations for fermion soliton stars,” [arXiv:2404.06979 \[gr-qc\]](#).
- [120] S. A. Teukolsky, “Perturbations of a rotating black hole. i. fundamental equations for gravitational, electromagnetic, and neutrino-field perturbations,” *The Astrophysical Journal* **185** (1973) 635–648.
- [121] S. A. Teukolsky and W. Press, “Perturbations of a rotating black hole. iii-interaction of the hole with gravitational and electromagnetic radiation,” *The Astrophysical Journal* **193** (1974) 443–461.
- [122] S. Chandrasekhar, *The mathematical theory of black holes*. 1985.
- [123] P. D. D’Eath, “Dynamics of a small black hole in a background universe,” *Phys. Rev. D* **11** (1975) 1387–1403.
- [124] E. Poisson, “Absorption of mass and angular momentum by a black hole: Time-domain formalisms for gravitational perturbations, and the small-hole / slow-motion approximation,” *Phys. Rev. D* **70** (2004) 084044, [arXiv:gr-qc/0407050](#).

- [125] M. V. S. Saketh, Z. Zhou, and M. M. Ivanov, “Dynamical Tidal Response of Kerr Black Holes from Scattering Amplitudes,” [arXiv:2307.10391](#) [[hep-th](#)].
- [126] M. M. Ivanov, Y.-Z. Li, J. Parra-Martinez, and Z. Zhou, “Gravitational Raman Scattering in Effective Field Theory: A Scalar Tidal Matching at $O(G^3)$,” *Phys. Rev. Lett.* **132** no. 13, (2024) 131401, [arXiv:2401.08752](#) [[hep-th](#)].
- [127] W. D. Goldberger and I. Z. Rothstein, “An Effective Field Theory of Quantum Mechanical Black Hole Horizons,” *JHEP* **04** (2020) 056, [arXiv:1912.13435](#) [[hep-th](#)].
- [128] W. D. Goldberger and I. Z. Rothstein, “Horizon radiation reaction forces,” *JHEP* **10** (2020) 026, [arXiv:2007.00731](#) [[hep-th](#)].
- [129] W. D. Goldberger and I. Z. Rothstein, “Virtual Hawking Radiation,” *Phys. Rev. Lett.* **125** no. 21, (2020) 211301, [arXiv:2007.00726](#) [[hep-th](#)].
- [130] A. Ross, “Multipole expansion at the level of the action,” *Phys. Rev. D* **85** (2012) 125033, [arXiv:1202.4750](#) [[gr-qc](#)].
- [131] E. R. Most, S. P. Harris, C. Plumberg, M. G. Alford, J. Noronha, J. Noronha-Hostler, F. Pretorius, H. Witek, and N. Yunes, “Projecting the likely importance of weak-interaction-driven bulk viscosity in neutron star mergers,” *Mon. Not. Roy. Astron. Soc.* **509** no. 1, (2021) 1096–1108, [arXiv:2107.05094](#) [[astro-ph.HE](#)].
- [132] E. R. Most, A. Haber, S. P. Harris, Z. Zhang, M. G. Alford, and J. Noronha, “Emergence of microphysical viscosity in binary neutron star post-merger dynamics,” [arXiv:2207.00442](#) [[astro-ph.HE](#)].
- [133] M. Alford, A. Harutyunyan, and A. Sedrakian, “Bulk Viscosity of Relativistic $n\text{p}\mu$ Matter in Neutron-Star Mergers,” *Particles* **5** no. 3, (2022) 361–376, [arXiv:2209.04717](#) [[astro-ph.HE](#)].
- [134] Y. Yang, M. Hippert, E. Speranza, and J. Noronha, “Far-from-equilibrium bulk-viscous transport coefficients in neutron star mergers,” *Phys. Rev. C* **109** no. 1, (2024) 015805, [arXiv:2309.01864](#) [[nucl-th](#)].
- [135] M. M. Ivanov, M. V. S. Saketh, and Z. Zhou *in preparation*.
- [136] G. B. Cook, S. L. Shapiro, and S. A. Teukolsky, “Rapidly rotating neutron stars in general relativity: Realistic equations of state,” *Astrophys. J.* **424** (1994) 823.
- [137] C. J. Krüger and K. D. Kokkotas, “Fast Rotating Relativistic Stars: Spectra and Stability without Approximation,” *Phys. Rev. Lett.* **125** no. 11, (2020) 111106, [arXiv:1910.08370](#) [[gr-qc](#)].
- [138] K. Chen and L.-M. Lin, “Fully general relativistic simulations of rapidly rotating quark stars: Oscillation modes and universal relations,” *Phys. Rev. D* **108** no. 6, (2023) 064007, [arXiv:2307.01598](#) [[gr-qc](#)].
- [139] C. Van Den Broeck and A. S. Sengupta, “Phenomenology of amplitude-corrected post-Newtonian gravitational waveforms for compact binary inspiral. I. Signal-to-noise ratios,” *Class. Quant. Grav.* **24** (2007) 155–176, [arXiv:gr-qc/0607092](#).
- [140] K. G. Arun, A. Buonanno, G. Faye, and E. Ochsner, “Higher-order Spin Effects in the Amplitude and Phase of Gravitational Waveforms Emitted by Inspiring Compact Binaries: Ready-to-use Gravitational Waveforms,” *Phys. Rev. D* **79** (2009) 104023, [arXiv:0810.5336](#) [[gr-qc](#)]. [Erratum: *Phys. Rev. D* **84**, 049901 (2011)].
- [141] C. K. Mishra, A. Kela, K. G. Arun, and G. Faye, “Ready-to-use Post-Newtonian Gravitational Waveforms for Binary Black Holes with Nonprecessing Spins: An Update,” *Phys. Rev. D* **93** (2016) 084054, [arXiv:1601.05588](#) [[gr-qc](#)].

- [142] K. Thorne, “Gravitational Radiation,” in *300 Years of Gravitation*, S. Hawking and W. Israel, eds., pp. 330. Cambridge University Press. 1987.
- [143] T. Damour, B. R. Iyer, and B. Sathyaprakash, “A Comparison of Search Templates for Gravitational Waves from Binary Inspiral,” *Phys. Rev. D* **63** (2001) 044023, [arXiv:gr-qc/0010009](#). [Erratum: *Phys.Rev.D* 72, 029902 (2005)].
- [144] A. Buonanno, B. Iyer, E. Ochsner, Y. Pan, and B. S. Sathyaprakash, “Comparison of Post-Newtonian Templates for Compact Binary Inspiral Signals in Gravitational-Wave Detectors,” *Phys. Rev.* **D80** (2009) 084043, [arXiv:0907.0700](#) [gr-qc].
- [145] S. Isoyama and H. Nakano, “Post-Newtonian templates for binary black-hole inspirals: the effect of the horizon fluxes and the secular change in the black-hole masses and spins,” *Class. Quant. Grav.* **35** no. 2, (2018) 024001, [arXiv:1705.03869](#) [gr-qc].
- [146] L. Blanchet, G. Faye, Q. Henry, F. Larrouturou, and D. Trestini, “Gravitational-Wave Phasing of Quasi-Circular Compact Binary Systems to the Fourth-and-a-Half post-Newtonian Order,” [arXiv:2304.11185](#) [gr-qc].
- [147] S. Khan, S. Husa, M. Hannam, F. Ohme, M. Pürrer, X. Jiménez Forteza, and A. Bohé, “Frequency-domain Gravitational Waves from Nonprecessing Black-hole Binaries. II. A Phenomenological Model for the Advanced Detector Era,” *Phys. Rev.* **D93** (2016) 044007, [arXiv:1508.07253](#) [gr-qc].
- [148] A. K. Mehta, A. Buonanno, R. Cotesta, A. Ghosh, N. Sennett, and J. Steinhoff, “Tests of general relativity with gravitational-wave observations using a flexible theory-independent method,” *Phys. Rev. D* **107** no. 4, (2023) 044020, [arXiv:2203.13937](#) [gr-qc].
- [149] **LIGO Scientific, Virgo** Collaboration, R. Abbott *et al.*, “Tests of general relativity with binary black holes from the second LIGO-Virgo gravitational-wave transient catalog,” *Phys. Rev. D* **103** no. 12, (2021) 122002, [arXiv:2010.14529](#) [gr-qc].
- [150] **LIGO Scientific, VIRGO, KAGRA** Collaboration, R. Abbott *et al.*, “Tests of General Relativity with GWTC-3,” [arXiv:2112.06861](#) [gr-qc].
- [151] A. K. Mehta, A. Buonanno, J. Gair, M. C. Miller, E. Farag, R. J. deBoer, M. Wiescher, and F. X. Timmes, “Observing Intermediate-mass Black Holes and the Upper Stellar-mass gap with LIGO and Virgo,” *Astrophys. J.* **924** no. 1, (2022) 39, [arXiv:2105.06366](#) [gr-qc].
- [152] J. Roulet, S. Olsen, J. Mushkin, T. Islam, T. Venumadhav, B. Zackay, and M. Zaldarriaga, “Removing degeneracy and multimodality in gravitational wave source parameters,” *Phys. Rev. D* **106** no. 12, (2022) 123015, [arXiv:2207.03508](#) [gr-qc].
- [153] M. Isi, K. Chatziioannou, and W. M. Farr, “Hierarchical test of general relativity with gravitational waves,” *Phys. Rev. Lett.* **123** no. 12, (2019) 121101, [arXiv:1904.08011](#) [gr-qc].
- [154] M. Saleem, N. V. Krishnendu, A. Ghosh, A. Gupta, W. Del Pozzo, A. Ghosh, and K. G. Arun, “Population inference of spin-induced quadrupole moments as a probe for nonblack hole compact binaries,” *Phys. Rev. D* **105** no. 10, (2022) 104066, [arXiv:2111.04135](#) [gr-qc].
- [155] K. G. Arun, B. R. Iyer, B. S. Sathyaprakash, and P. A. Sundararajan, “Parameter Estimation of Inspiralling Compact Binaries Using 3.5 Post-Newtonian Gravitational Wave Phasing: The Non-spinning Case,” *Phys. Rev.* **D71** (2005) 084008, [arXiv:gr-qc/0411146](#) [gr-qc]. [Erratum: *Phys. Rev.D*72,069903(2005)].
- [156] T. Damour, B. R. Iyer, and B. S. Sathyaprakash, “Improved Filters for Gravitational Waves from Inspiralling Compact Binaries,” *Phys. Rev.* **D57** (1998) 885–907, [arXiv:gr-qc/9708034](#) [gr-qc].
- [157] T. Damour and A. Nagar, “Comparing Effective-One-Body gravitational waveforms to accurate

- numerical data,” *Phys. Rev. D* **77** (2008) 024043, [arXiv:0711.2628 \[gr-qc\]](#).
- [158] S. Husa, S. Khan, M. Hannam, M. Pürrer, F. Ohme, X. Jiménez Forteza, and A. Bohé, “Frequency-domain Gravitational Waves from Nonprecessing Black-hole Binaries. I. New Numerical Waveforms and Anatomy of the Signal,” *Phys. Rev. D* **93** (2016) 044006, [arXiv:1508.07250 \[gr-qc\]](#).
- [159] R. Geroch, “Multipole Moments. II. Curved Space,” *J. Math. Phys.* **11** (1970) 2580.
- [160] R. Hansen, “Multipole Moments of Stationary Spacetimes,” *J. Math. Phys.* **15** (1974) 46.
- [161] K. Thorne, “Multipole Expansions of Gravitational Radiation,” *Rev. Mod. Phys.* **52** (1980) 299–339.
- [162] S. Taylor and E. Poisson, “Nonrotating Black Hole in a Post-Newtonian Tidal Environment,” *Phys. Rev. D* **78** (2008) 084016, [arXiv:0806.3052 \[gr-qc\]](#).
- [163] K. Chatziioannou, E. Poisson, and N. Yunes, “Tidal heating and torquing of a Kerr black hole to next-to-leading order in the tidal coupling,” *Phys. Rev. D* **87** no. 4, (2013) 044022, [arXiv:1211.1686 \[gr-qc\]](#).
- [164] K. Chatziioannou, E. Poisson, and N. Yunes, “Improved next-to-leading order tidal heating and torquing of a Kerr black hole,” *Phys. Rev. D* **94** no. 8, (2016) 084043, [arXiv:1608.02899 \[gr-qc\]](#).
- [165] M. Maggiore, *Gravitational Waves. Vol. 1: Theory and Experiments*. Oxford University Press, 2007.